Influence of Neutron Scattering and Source Extent on the Measurement of Neutron Energy Spectra at ASDEX

K. Hübner [1], B. V. Robouch [2], R. Bätzner [1], M. Roos [1], L. Ingrosso, H. Wurz, ASDEX Team

IPP III/122 August 1987

MAX-PLANCK-INSTITUT FÜR PLASMAPHYSIK

8046 GARCHING BEI MÜNCHEN

MAX-PLANCK-INSTITUT FÜR PLASMAPHYSIK

GARCHING BEI MÜNCHEN

Influence of Neutron Scattering and Source Extent on the Measurement of Neutron Energy Spectra at ASDEX

K. Hübner [1], B. V. Robouch [2], R. Bätzner [1], M. Roos [1], L. Ingrosso, H. Wurz, ASDEX Team

IPP III/122 August 1987

1) Institut für Angewandte Physik II, Universität Heidelberg
Albert-Überle-Straße 3-5, D-6900 Heidelberg

2) Associazione EURATOM-ENEA sulla Fusione
Centro Ricerche Energia,
C.P.65, I-00044 Frascati (Roma), Italy

Die nachstehende Arbeit wurde im Rahmen des Vertrages zwischen dem Max-Planck-Institut für Plasmaphysik und der Europäischen Atomgemeinschaft über die Zusammenarbeit auf dem Gebiete der Plasmaphysik durchgeführt.

This is a cooperative work by MPI für Plasmaphysik, Universität Heidelberg, and ENEA

Contents

1) Introduction

All neutron diagnostics inside the hall of a tokamak are strongly influenced by neutron scattering in the materials of the tokamak device. Furthermore many neutron diagnostics require a well-defined direction of neutron incidence and hence suffer from the large extent of the neutron source in a tokamak. Diagnostic systems must therefore be shielded against scattered neutrons, and collimators have to be used to define the pencil of neutrons impinging on the detection system. Neither can be done perfectly and in most situations it is impossible to investigate the remaining influences experimentally. But an unknown background of scattered neutrons and spectral broadening due to the source extent can lead to misinterpretations of the results. There is thus a great need for numerical studies in this field.

Such numerical investigations must yield the angle-dependent spectral neutron fluences arriving at a given point or region of interest as well as the contributions of the different parts of the facility to these spectral fluences. The first is needed to calculate the response of the neutron detector, the second to identify the main scatterers of the background fluence in order to define optimized experimental setups. The neutron transport codes widely used as well as albedo calculations cannot deliver this information. We therefore had to use the VINIA-3DAMC software, which provides all these and even more data.

We consider the problem of nuclear emulsion measurements at ASDEX. Besides the application of the VINIA-3DAMC software, this needs a description of the plasma neutron source, a model of the ASDEX structure, and calculation of the response of the nuclear emulsion to the incoming spectral neutron fluence. The latter is essential for comparing the numerical results with measurements at ASDEX. To treat this part, we developed the NEPMC software.

The aim of the present work is not to give a detailed solution to all problems involved, but to demonstrate the feasibilty, reliability and usefulness of the method. We therefore used simplified treatments for the ASDEX model, the plasma neutron source and the track statistics in the NEPMC software, which are now to be improved. It should be pointed out, however, that such calculations are of interest not only for nuclear emulsion measurements as well as any other neutron diagnostics, but also for all problems of neutron shielding for other diagnostics.

2) Plasma model

The plasma neutron source is described by local values for the neutron yield and the neutron energy spectrum. For the investigations reported here, these values are determined from the ASDEX data sets obtained for shots no. 16910 and 19111. Both are discharges of the H-type, no. 16910 with neutral injection of deuterium in deuterium plasma and no. 19111 with neutral injection and ICRH. We take the plasma parameters during the flat top of the neutron pulse as representative of the whole duration of the neutron production. They are:

shot number	16910	19111	
plasma current	320.0	384.0	kA
major plasma radius	166.5	169.3	cm
Shafranov shift	9.1	9.2	cm
minor plasma radius	40.0	40.0	cm
mean electron density	2.4	2.9	10^{13} cm^{-3}
central electron temperature	1.46	2.73	keV
central deuteron temperature	2.0	3.72	keV
ICRH power	-	0.9	MW
neutral injection power	3.1	3.6	MW
neutral injection energy	44.6	44.6	keV
neutron yield	1.3	3.2	10^{13} neutrons
thermonuclear component	4.9	24.2	%

The deposition profile for the fast deuterons is calculated with the FREYA code. The deuteron temperature is determined with our interpretation code for the neutron rate [1], which also delivers the emission profiles both for thermonuclear neutrons and for neutrons produced by the injected particles.

The neutron energy spectrum of the thermonuclear component is easily determined from the deuteron temperature. It is assumed that for neutral injection the ion temperature has the same radial profile as the electron density. The energy spectrum of beam-produced neutrons is determined by the stationary energy distribution of the injected deuterons. This distribution is assumed to be determined by the classical energy relaxation time. We use the same approximation in our interpretation code, and it proved to hold well for the ASDEX plasma parameters.

So far our plasma model contains all the available information. A simplification is made concerning the motion of the fast deuterons; during their energy

relaxation time they are assumed to stay on their flux surface and simply move on closed toroidal circles on this surface instead of following the twisted magnetic field lines. The pitch angle of the magnetic field lines is small in the region of the bulk of neutron production and will not lead to any remarkable broadening of the neutron spectrum. In our calculations the neutron energy is thus simply determined by the angle between the normal to the poloidal plane of emission and the direction of emission. - More serious may be the neglect of the gyration of fast deuterons around their field line, but for this motion no detailed data are available.

3) ASDEX model

The main components of the ASDEX facility were modelled for input to the VINIA software in a simplified manner by using plane and quadratic surfaces and D-shaped contours of revolution. In the standard calculations our ASDEX model now contains the vacuum chamber with a quartz window and its support, the 16 toroidal coils, the ohmic coils, the central core of 3 cylindrical regions, the collimator for exposing and shielding the nuclear emulsion, and the Ilford glass supporting the nuclear emulsion. In a few calculations we also investigated the effect of some of the components of the divertor. For two special runs the space between the toroidal coils was filled to different degrees with Al and Fe to simulate the effect of the different diagnostic equipment installed around ASDEX. In two other special runs the strengthened concrete walls, the floors, the wooden roof of the ASDEX hall, and the air in the hall were also taken into account.

We use a Cartesian coordinate system with the origin at the centre of the tokamak, the x-y plane being the horizontal plane and the x-axis collinear with the port window axis. The vacuum chamber and all coils were approximated by D-shaped contours of revolution. Figures 3.1 to 3.4 present the following cross-sections:

1) vertical-axial through a toroidal field coil,
2) same for the real ASDEX for comparison,
3) horizontal-equatorial (x-y plane), and
4) vertical-axial (x-z plane) through the centre of the nuclear emulsion.

Figure 3.5 shows the ASDEX model with the hall and the area in the control room which we will consider later.

In our model, for each different region a homogeneous nuclide composition is assumed; in the case of a polymaterial structure a homogenized mixture of the components is used. Table 3.1 gives the composition densities in $(cm\ barn)^{-1}$ used in our calculations.

We consider measurements with two different collimators, viewing the plasma radially; collimator 1 for discharge no. 16910 in front of a large port closed with a quartz window, and collimator 2 for discharge no. 19111 beside a toroidal field coil in front of the vessel wall.

Figure 3.6 gives the horizontal and vertical cross-sections of the collimator 1, including the nuclear emulsion, in order to illustrate three different zones which are essential for the discussion of the results. These zones are defined by the position of the nuclear emulsion and the shape of the collimator. Zone 1 is the free aperture of the collimator; it is defined by the pencil of lines from the considered point of the nuclear emulsion to the plasma which do not touch the collimator. Zone 2 is the zone of reduced shielding of the collimator due to the indented structure of its opening; it is defined by the pencil of lines from the nuclear emulsion to the plasma which do see the dent inside the collimator. Zone 3 is the region of full shielding by the collimator material. In the figures the three zones are shown for the central point of the emulsion; they change somewhat from point to point of the emulsion.

The nuclear emulsion is located in the x-z plane (figure 3.6). The glass support is $2.5 \times 7.5\ cm^2$, but the scanned part of the emulsion is limited to only $1.5 \times 4.5\ cm^2$.

Figure 3.7 gives the horizontal and vertical cross-sections of collimator 2. Here for simplicity we have considered in the calculations only zone 1. Zone 2 was included in zone 3.

4) VINIA-3DAMC software

The VINIA software [2] is a numerical facility aimed at carrying out numerical experiments on problems of migration of neutrons through matter. The VINIA software structure may best be described as consisting of a "back bone" invariant strict Monte Carlo coupled to a problem-specific information-extracting part. It is thus by no means a "black box" numerical code solving routine problems, but a flexible tool designed for numerical experiments.

The analogical Monte Carlo "back bone" strictly follows the probabilistic migration and interaction of a neutron in the space adjacent to the emission region, starting from the birth of the neutron right to its extinction. To do so the VINIA software relies on Nuclear Data Bank (NDB) files in ENDF/B4 format, using the data as given "in extenso". It does not use truncation (of, for example, Legendre polynomials, which would lead to negative probabilities), approximations, discretization of either energy (no group pretreatment) or space (no ray effects); space and energy are continua in the treatment. The nuclear data precision is thus that of the NDB files unimpaired by software treatments. The tabulated data are just taken "in extenso" with linear interpolation between the specified pointwise represented data.

The neutrons are emitted within the plasma region, reproducing probabilistically the required nonhomogeinity for the position, and the imposed anisotropy of direction and energy, corresponding to the plasma data as specified in section 2. For illustration figures 4.1 and 4.2 show the toroidal and poloidal distributions of the points of birth calculated for 5000 neutrons. The Shafranov shift of the plasma axis is clearly seen in the poloidal plane.

Subsequently, the history of the neutron migration is followed probabilistically to the position of the next collision within the surrounding material space. At this point the nature of the collided nuclide, the branch of the reaction followed, and the re-issuing neutron direction and energy are randomly determined with allowance for the anisotropy of the collision and - in the case of a reaction with continuum energy - for the spectrum as given by the NDB files. The process is then reiterated until the neutron is either absorbed in the reaction or attenuated below a significant value through loss to the external space, or if its energy drops below a cut-off value below which the neutron reactions are of no interest to the problem under study.

To ensure history contributions to the nuclear emulsion in spite of the negligible volume of the detecting system as compared wih the scattering volume of the facility, we use the "flux-at-point" method: at each collision in the system contributions at the emulsion are recorded as equal to the probabilities of neutrons being scattered from the point of collision into the emulsion position, this being done for each of the possible reaction channels.

To account for the extent of the nuclear emulsion within the shielding collimator with the consequent variation in the size and shape of the three zones, the detecting point is randomly varied from emitted neutron to emitted neutron along the scanned emulsion area, thus simulating the average exposure in the emulsion.

To avoid numerous fast neutron exits through thin walls, the "forced collision" method is applied. From a neutron package W_0 proceeding in a given direction, a part

$$W(L) = W_0 \exp\left(-\int_0^L n\sigma \, dl\right)$$

escapes without collisions. Here L is the smallest distance in the given direction after which the product $n\sigma$ of the density and cross-section remains 0. The remaining part $W_0 - W(L)$ undergoes a collision at a certain point $x = \langle 0, L \rangle$ determined by

$$p = \frac{W_0 - W(x)}{W_0 - W(L)},$$

which becomes the starting point for the next iteration step. Here p is a random number between 0 and 1.

Owing to the extent of the ASDEX facility and the selectivity of the collimator, many of the neutrons, while consuming their share of computation CPU time, contribute only marginally to the detected signal. To reduce the CPU time devoted to weakly contributing histories, we resort to a "weighted emission" in two different regions, which are shown in figure 4.1: a small one in front of the collimator and a larger one for the rest of the plasma. We use an equal random probability of birth in the two regions, with a starting weight proportional to their respective volumes. A centre angle of $\pm 30^{\circ}$ for the smaller region ensures a balanced and adequate statistical study of neutrons in each region.

Our first results indicated that the total neutron fluences arriving at the emulsion strongly depends on the number of neutrons emitted in zone 1. Now, with 1000 emitted neutrons 500 are of course emitted in the region of $\pm 30^{\circ}$ in front of the collimator, but in zone 1 there are only 79 neutrons and this number has a statistical error of 11%. In later runs we therefore restricted the smaller region in the weighted emission to $\pm 10^{\circ}$.

From the first results it also appeared that strong contributions to the collided neutron fluence arriving at the emulsion originate in the material between plasma and emulsion. To ensure a proper filling of the distribution of such events we introduced a "beamed emission" into two complementary regions with equal random probability of emission and a starting weight coefficient proportional to the respective solid angles of the two regions as seen from the point of birth of the neutron. The solid angles are determined by a sphere around the centre of the material region of interest. For collimator 1 this is the quartz window and for collimator 2 the collimator itself, including thus an appropriate part of the vessel in this solid angle.

5) NEP and NEPMC software

In nuclear emulsions the neutrons are detected by recoiled protons. One measures the length of the proton tracks and their angle with respect to the direction of incidence of the neutrons. The nuclear emulsion is aligned with its axis along the central line of sight of the collimator and all angles are measured with respect to this axis. Owing to the large extent of the neutron source and the finite aperture of the collimator the neutrons cover a certain range of angles of incidence.

The proton energy is determined from the length of the tracks and then the neutron energy is calculated from the proton energy E_p and scattering angle Θ by the relation $E_n = E_p \cos^2\Theta$ and is thus distorted by the spread in the angles of neutron incidence.

Our NEP software analytically calculates the proton energy spectrum (P-spectrum) and the apparent neutron energy spectrum (N^*-spectrum) for a given energy and direction of incoming neutrons. To demonstrate the effects, figure 5.1

shows for a monoenergetic neutron fluence of 2.45 MeV the resulting proton and neutron energy spectra for different angles α of incidence. Furthermore it is taken into account that in scanning nuclear emulsions the maximum scattering angle of the tracks used is, for different reasons, limited to a certain value Θ_{max}, which is usually taken between 10^o and 30^o.

The resulting neutron spectrum is essentially broadened and the integral value over the spectrum, i.e. the apparent neutron fluence is reduced by the factor $\cos\alpha$. This broadening is to be considered as one contribution to the response function of the nuclear emulsion caused by the size of the source and the maxiumum scanning angle Θ_{max}.

The advantage of the analytical NEP software is that the whole set of energy channels is filled at each incoming neutron just as it contributes by its dispersion probability cloud. At the same time a corresponding inversion serves to fill the energy channels of the N^*-spectra. However, the response function of a neutron detector is also essentially determined by the inherent measuring errors. In the case of a nuclear emulsion these are the errors in measuring track length and scattering angle as well as the errors introduced by range straggling and variation of the emulsion thickness.

All these effects are taken into account in our NEPMC software, which is a Monte Carlo code. In this software, for each incoming neutron with given energy and angle of incidence, a number of proton tracks (input parameter) is randomly generated and their length and angle are stochastically perturbed by means of Gaussian distributions with standard deviations previously determined experimentially in test measurements with the emulsions.

In order to demonstrate the effects of these errors, figure 5.2 shows the same spectra as figure 5.1, now calculated with the NEPMC software. Owing to the line broadening caused by the emulsion, the off-axis broadening becomes noticable only for incidence angles above 1^0. In figure 5.3 the results of NEPMC calculations for a monoenergetic neutron source are compared with measurements made at the Gothenburg accelerator for two different maximum scanning angles Θ_{max}. We must point out here that our treatment of proton track statistics is rather approximative, and so it must be checked in greater detail in a further work against test measurements with accelerators.

6) General description of output

6.1) Discussion of the three zones

The presentation of the results starts with a physical discussion of the different contributions to the neutron fluence arriving at the emulsion from the three zones defined in section 3.

Zone 1 defines the part of the plasma we want to observe. In this zone we have first the flux of emitted neutrons, which gives the desired signal at the detector. Then there is a flux of collided neutrons, which originates firstly from the inner part of the vessel, the ohmic coils and the core, secondly from the quartz window, and thirdly from the collimator. This scattered flux in zone 1 imparts an unavoidable background to the measured neutron spectrum.

Zone 2 is the region of reduced shielding. It may be considered as the region of "soft edges" of the collimator. Owing to the extent of the nuclear emulsion it is unavoidable too, but it may be reduced by improved design of the collimator. In zone 2 we thus have a reduced flux of emitted and collided neutrons as a "shine-through" of the collimator. Here also the outer part of the vessel contributes to the collided flux.

Zone 3 is the region shielded by the collimator. Here, after strong attenuation, a residual flux of emitted neutrons reaches the detector as well as a collided flux consisting of the attenuated fraction of the neutron flux at the position of the collimator and finally the collided flux produced inside the collimator itself.

6.2) Output of the VINIA calculations

The numerical calculation with the VINIA software delivers for each emitted neutron first the position of birth and - when we consider the full size of the emulsion - the position of the selected point in the emulsion for that particular history. Furthermore, it gives the energy and weight of the emitted neutron, successively the coordinates of all points of collision and for each collision the energy and weight of all contributions at the selected point of the emulsion. All these data are stored in PTO files for further investigations. Simultaneously during the same run we calculate the neutron fluence arriving at the emulsion

as well as the fluence that would reach the emulsion if the quartz window or collimator (depending on the zone) and the Ilford glass support had been absent.

At present the following neutron energy spectra are being calculated:
#1 total neutron spectrum at the nuclear emulsion
#2 same without attenuation in the Ilford glass
#3, #4, #5 spectra of emitted neutron fluence in zones 1, 2, 3
#6 same as #3 on the assumption that no quartz window is present
#7, #8 same as #4, #5 on the assumption that no collimator is present
#9, #10, #11 spectra of collided neutron fluence in zones 1, 2, 3
#12 same as #9 on the assumption that no quartz window is present
#13, #14 same as #10, #11 on the assumption that no collimator is present.

Also calculated are the integral values for these 14 spectra as well as the integral values of the emitted neutron fluences in the three zones. All neutron fluences are normalized to the number N_e of emitted neutrons. We call them specific or normalized fluences (neutrons/cm^2 per emitted neutron) to distinguish them from the neutron fluence (neutrons/cm^2) arriving physically at the emulsion. These fluences are the product of the specific fluences times the total neutron yield, which is an experimental value of no importance to the VINIA calculations. They are to be used for comparison with the experimental results.

Correspondingly, the neutron energy spectra are given as specific neutron fluences per MeV for discussion of the numerical results and in neutrons/cm^{2}MeV for comparison with experimental results in section 9.

6.3) Output of the NEPMC calculations

Spectrum #1 is taken as input for the NEP software, which delivers 6 additional spectra:
#15, #16, #17, proton energy spectra, $\Theta_{max} = 10^0, 20^0, 30^0$ respectively, and
#18, #19, #20, neutron energy spectra $\Theta_{max} = 10^0, 20^0, 30^0$ respectively.
It is recalled that the NEP calculations only contain the effect of off-axis incidence of neutrons onto the emulsion, which results in a broadening of the spectrum but reduces the scattered background owing to the limited scanning angle Θ_{max}. The PTO files created are then used as input to the NEPMC software to take into account also the spectral broadening due to the errors in proton track measurement. We calculate P-spectra and N^*- spectra for desired

values of Θ_{max} which are to be compared with the measured spectra. As already mentioned in section 5, the integral values of the N^*-spectra, i.e. the apparent neutron fluences which are measured by the emulsion, must be smaller than the corresponding values from the VINIA calculations.

It turned out that the NEP calculation included in the VINIA calculations consumes about 2/3 of the CPU time. It was hence decided to exclude this part of the program and to calculate the proton and neutron spectra from the PTO files by using off-line the NEPMC software, which is much faster.

6.4) Other outputs

Complementary information regarding the migration and interaction of neutrons, such as nuclides, type of reaction and activation in different material parts of the ASDEX structure, are stored and in our runs serve to clarify the importance and particularities of different materials. They are not presented here because they do not have a direct bearing on the problem of emulsion measurements.

7) Results of the standard case

In this section we discuss the results of our standard calculation for ASDEX discharge no. 16910 with collimator 1 using 34,775 emitted neutrons and the input parameters for the plasma neutron source and ASDEX model as described in sections 2 and 3.

7.1) Neutron fluence

The total specific neutron fluence arriving at the nuclear emulsion (#1) is

$$0.279 \times 10^{-7} \pm 2.8\% \text{ neutrons/cm}^2 \text{ per emitted neutron,}$$

which is by a factor of 1.92 larger than the desired fluence of emitted neutrons in zone 1.

The contributions of the different zones to the total specific fluence are

emitted neutrons,	zone 1 (# 3):	$0.145 \times 10^{-7} \pm 2.2\%$	i.e. 52.0 %
	zone 2 (# 4):	$0.244 \times 10^{-8} \pm 4.6\%$	8.8 %
	zone 3 (# 5):	$0.656 \times 10^{-11} \pm 3.2\%$	0.02 %
collided neutrons,	zone 1 (# 9):	$0.867 \times 10^{-8} \pm 7.9\%$	31.1 %
	zone 2 (#10):	$0.201 \times 10^{-8} \pm 6.1\%$	7.2 %
	zone 3 (#11):	$0.248 \times 10^{-9} \pm 38.4\%$	0.9 %

The large uncertainty of the contribution of collided neutrons in zone 3 is caused by poor filling of the distribution for the rare collisions inside the collimator material. Yet this has no consequence since the contribution remains negligible as compared with the other ones.

Of great interest are the specific fluences arriving at the collimator, i.e. the fluences to which an unshielded detection system would be exposed at this place. We find for

emitted neutrons, all zones: 0.629×10^{-7}

collided neutrons, all zones: 1.700×10^{-7}

It is remarkable that the collided fluence arriving at the collimator is more than one order of magnitude larger than the desired fluence of emitted neutrons in zone 1.

The numerical results may be checked against analytically calculated values. Approximative analytical values for the emitted neutron fluence in the three zones and their mean attenuation in the quartz window and the collimator are easely calculated assuming a neutron line source on the plasma axis and a punctiform nuclear emulsion. For simplicity here we consider only the neutron emission in the front half of the tokamak, i.e.for positive x-values. We find the following results:

Specific emitted neutron fluence without attenuation

zone	analytical value	numerical value
1	0.281×10^{-7}	$0.265 \times 10^{-7} \pm 2.2\%$
2	0.286×10^{-7}	$0.300 \times 10^{-7} \pm 2.2\%$
3	2.891×10^{-7}	$2.895 \times 10^{-7} \pm 1.1\%$
total	3.458×10^{-7}	$3.460 \times 10^{-7} \pm 0.9\%$

Attenuation factor:	analytical value	numerical value emitted neutrons	numerical value collided neutrons
quartz window	1.6	1.82 ± 3.1%	0.71 ± 12.0%
collimator, zone 2	7.0	7.56 ± 5.1%	13.05 ± 8.1%
collimator, zone 3	6614	2738 ± 4.1%	555 ± 38.5%

In estimating the analytical values for the attenuation we used mean values for the total cross-section for a spectrum near 2.45 MeV (figure 7.1). The numerical values are the ratio of the considered neutron fluences without and with quartz window or collimator. The results for emitted neutrons agree well with the analytical values for zone 1 and 2. The discrepancy for zone 3 corresponds to an error of only 10% in the product of the mean value for the cross-section and path length in the collimator material. The results for collided neutrons will be discussed together with the neutron spectra.

7.2) Neutron spectra

For the standard-case calculation figure 7.2 shows spectrum #1, which gives the specific spectral neutron fluence arriving at the nuclear emulsion. Its 6 components, namely spectra #3 to #5 and #9 to #11 of emitted and collided neutrons in the three zones as defined in section 6.2, are shown in figure 7.3. Furthermore figure 7.4 gives spectra #6 to #8 and #12 to #14 of the neutron fluences entering the emulsion if no quartz window or collimator is present.

Figure 7.2 also shows spectrum #1 plus and minus one standard deviation, evidencing the statistical relevance of the broad foot below the main line around 2.45 MeV and the uncertainty in the neutron fluence below 2 MeV.

Spectra #3 to #5 of the emitted neutrons show a characteristic change from zone 1 to zone 3. In zone 1 the observation is mainly perpendicular to the direction of motion of fast deuterons and therefore the spectrum is centred around 2.45 MeV. In zone 2 the observation of neutrons is slightly in the forward and backward directions, causing a double-humped spectrum owing to the dependence of the neutron energy on the emission angle. This effect is further enhanced in zone 3. The remaining emission near 2.45 MeV is due to thermonuclear production, which in the case considered here amounts to only 4.9% of the total neutron production (see section 2) with a consequently large statistical fluctuation in the results. - If necessary, this fluctuation can be suppressed by a weighted emission of both contributions to neutron production.

All spectra of collided fluences show a broad contribution between 2.2 MeV and the maximum possible neutron energy of 2.7 MeV, a minimum at about 1.8 MeV and an increasing contribution at lower energies. Spectra #9 and #10 show a slightly reduced ratio of the low and high-energy parts compared with the unshielded spectra #12 and #13. This is due to the increase in the cross-section of PE for decreasing energy below 2.45 MeV.

It is of interest to consider the relation of emitted to collided neutron fluences at the emulsion in the three zones:

	zone 1	zone 2	zone 3
without window	4.35	-	-
without collimator	-	0.71	0.13
with both	1.79	1.23	0.026

The part of the fluence in zone 1 incident on the quartz window contains about 4 times as many emitted as collided neutrons; this ratio is deteriorated essentially in the quartz window. In fact, the incoming fluence onto the quartz window consists not only of the neutron fluence originating in zone 1 from the plasma and the inner parts of the vessel but also of a large fluence of emitted neutrons from the rest of the plasma as well as collided neutrons from all directions; the last may be of the order of the collided fluence at the collimator.

The generation of a collided fluence in the quartz is also evidenced by the decrease in the "attenuation" for collided neutrons as compared with the values for emitted neutrons. The same observations hold for the collimator in zone 3, both for the decrease of the ratio of emitted to collided fluence and for the decrease in "attenuation".

In zone 2 we found, as discussed above, an increase in "attenuation" due to the energy dependence of the cross-sections and this corresponds here to an increase in the ratio of emitted and collided fluence upon inserting the collimator.

7.3) Neutron spectra calculated with NEPMC

Figure 7.5 gives spectrum #1 in four different shapes. Figure 7.5a is the spectral fluence as it arrives at the emulsion; this is the output of the VINIA calculation. Figure 7.5b gives the output of the NEP calculations (spectrum #19) made for only 10775 emitted neutrons. This spectrum now includes the effects of the extension of the neutron source and is therefore somewhat broadened. Figure 7.5c gives the results of the NEPMC calculations using all emitted neutrons; it is essentially broadened owing to the statistical processes in the emulsion and the errors in track measurement. Finally, figure 7.5d gives the same spectrum smoothed over 100 keV in order to compare it with the experimental results.

Figure 7.6 shows the proton energy spectra as well as the apparent neutron energy spectra calculated by the NEP software from the VINIA results for different maximum scanning angles Θ_{max}. The low energy limit in the proton spectra is determined by this angle and a scanning limit for the track length. The results for the neutron spectra demonstrate the detoriation of energy resolution with increasing Θ_{max}.

Figure 7.7 shows the components of the emitted and collided fluence in the three regions; they are just the NEPMC versions of the spectra in figure 7.3. Figure 7.8 gives the same spectra as for 7.7 but now all with the same scale to show more clearly the relations between emitted and collided fluences in the three zones. In particular, it demonstrates that zone 3 is well shielded and proper design of the collimator will reduce the contributions in zone 2.

The local calculation of collisions in the VINIA software and the storage of all relevant data in the PTO files allows us to calculate with the NEPMC software the separate contributions of the different materials to the collided neutron fluence in each of the three regions. We find the following results for the neutron fluence per emitted neutron (in 10^{-9} neutron/cm^2):

	zone 1	zone 2	zone 3	all zones
vessel	1.67	0.50	0.042	2.22
ohmic coils	0.62	0.10	0.0007	0.71
toroidal field coils	0.10	0.027	0.0085	0.13
quartz window	6.41	1.13	0.0011	7.54
window support	0.49	0.64	0.0013	1.14
collimator	-	0.028	0.12	0.14

These numbers demonstrate, firstly, that the main contribution to the collided fluence comes from zone 1 and is therefore unavoidable and, secondly, that the predominant scatterer is the quartz window. It should be mentioned here that owing to the statistical errors the total collided fluence from the NEPMC calculation will always slightly differ from the original VINIA result. The systematic reduction caused by the off-axis incidence of neutrons in this particular situation for zone 1 is small compared with the statistical effects, only for the collided neutrons in zone 3 this reduction is 40% because these neutrons enter the emulsion with large angles α.

Figures 7.9 and 7.10 give the spectra of the collided fluence from the 6 regions of ASDEX summed over all 3 zones. They show that the main part of the collided fluence is only slightly shifted to lower energies as compared with the spectrum of emitted neutrons and will thus cause essential broadening or even an additional hump at the low-energy wing of the neutron spectrum. At lower neutron energies the collided fluence decreases very fast; but below 1.5 MeV we have strong contributions from (n,n') reactions on heavy nuclides which have a strong anisotropic cross-section and energy levels in the range of 0.7 to 1.1 MeV.

8) Results for collimator 2

For ASDEX discharge no. 19111 with collimator 2 we used only 3600 emitted neutrons in the VINIA calculations and 3999 in NEPMC. The aim of these calculations was mainly to apply our method to another situation with respect to the plasma data, the position an design of the collimator and the material intervening between the plasma and emulsion. In fact, the material wall in front of the collimator is now the stainless steel of the vessel instead of the quartz window. For simplicity, here we only distinguished two zones. Zone 1 is again the free aperture of the collimator. Zone 2 is included in zone 3. Here the Ilford glass plate was not introduced, and so its absorption has to be taken into account when comparing the numerical results with the experimental ones.

8.1) Neutron fluence

The total specific neutron fluence arriving at the emulsion is now

$$0.115 \times 10^{-6} \pm 8.1\% \text{ neutrons/cm}^2 \text{ per emitted neutron.}$$

For different reasons it is larger than the specific fluence in collimator 1. First of all the absorption of the Ilford glass will reduce it to 0.099×10^{-6}; but the main effect is due to the larger aperture and the smaller distance between the plasma and collimator.

The contributions of the different zones to the total specific neutron fluence are:

emitted neutrons,	zone 1 (#3)	0.584×10^{-7}	± 6.5 %	i.e. 50.6 %
	zone 3 (#5)	0.007×10^{-7}	± 38.5 %	0.6 %
collided neutrons,	zone 1 (#9)	0.531×10^{-7}	± 15.7 %	46.0 %
	zone 3 (#11)	0.033×10^{-7}	± 19.5 %	2.8 %

and the specific fluences arriving at the emulsion if the collimator is not present are:

emitted neutrons, all zones	1.980×10^{-7}
collided neutrons, all zones	4.197×10^{-7}.

The shine-through of collimator 2 for emitted neutrons is essentially reduced as compared with collimator 1. Here we use a slanting pyramid-shaped cut-out, instead of the step in collimator 1. We used a punctiform nuclear emulsion, however, and therefore the shine-through is underestimated. Even in collimator 2 the collided fluence mainly enters through zone 1 and it is larger than for collimator 1, this being caused - as we shall see from the spectra - by the short distance to the vessel. The attenuation factors for the collimator here are 204 for the emitted neutrons and 112 for the collided neutrons.

As there is a lack of space near the ASDEX facility at the position of this collimator, the effective shielding thickness of the collimator walls is smaller than in collimator 1. Nevertheless - as seen above - it sufficiently reduces the collided fluence in zone 3, namely to 3.4% of the total fluence at the emulsion, which is by no means a problem when compared with the collided fluence entering through zone 1. The attenuation here is also smaller for the collided fluence than for the emitted fluence, evidencing once more the production of collided fluence in the collimator material.

8.2) Neutron spectra

Figure 8.1a shows spectrum #1, which is the total specific spectral fluence arriving at the nuclear emulsion. In figure 8.1b the two lines corresponding to one standard deviation are shown. Owing to the small number of emitted neutrons the statistical error in the foot below the main line is larger than in the standard calculation. Figure 8.2 gives the 4 components, namely spectra #3 and #5 of emitted and #9 and #11 of collided neutrons. It is necessary to explain

the shape of the spectrum of emitted neutrons in zone 3. The large peak at 2.45 MeV is caused by thermonuclear production, which amounts to 24.2% in the discharge. The broad line at lower energies is produced by neutrons emitted backwards to the direction of the injected deuterons. The symmetric high-energy wing from forward emission is totally absorbed in the toroidal field coil on which the collimator is mounted.

In figure 8.2 we also have spectra #8 and #14 for the emitted and collided fluences as they would arrive at the emulsion if there had been no collimator. In spectrum #8 a small contribution from the forward emission of injection-produced neutrons is seen; this arrives at the emulsion, missing on the right-hand side the toroidal field coil. In reality, they are then absorbed in the collimator.

8.3) Neutron spectra calculated with NEPMC

Figure 8.3 gives the NEPMC output for spectrum #1 and its emitted and collided fluence components. They do not differ in their spectral shapes from the results for collimator 1. In figure 8.4 we have the spectral contributions from the vessel, the ohmic coils, toroidal field coils and the collimator material to the collided neutron fluence and in figure 8.5 the contribution from the vessel compared with the sum of all the other parts. The integral values are:

vessel	51.90×10^{-9}
ohmic coils	3.13×10^{-9}
toroidal field coils	0.45×10^{-9}
collimator	1.20×10^{-9} .

Here the reduction of fluence caused by the off-axis incidence of neutrons is 60% for the neutrons in zone 3. This effect is demonstrated in fig 8.6 . We have in fig 8.6a the spectrum of neutrons collided in the toroidal field coil, which enter the emulsion more or less from the side. If we do not take the real angle of incidence into account but calculate the spectrum assuming incidence along the collimator axis, we get the spectrum in figure 8.6b. This illustrates for an extreme situation the selective response of the nuclear emulsion to the angle of incidence, which in the case considered here reduces the scattered background to 18%. Furthermore it obviously demonstrates the necessity of obtaining from the neutron migration code the angle dependence of the spectral neutron fluence at the detector. Without this information here we would expect the spectrum in figure 8.6b instead of that in figure 8.6a for the response of the nuclear emulsion.

9) Comparison with experimental results

9.1) Neutron fluence

In this section we compare the numerical results with the measured ones. From the proton track density in the emulsion we obtain the neutron fluence at the emulsion. Furthermore, the total neutron yield is measured by counters, and thus we can derive specific neutron fluences from the emulsion measurements or neutron fluences from the VINIA-NEPMC results. We find:

ASDEX discharge	no. 16911 collimator 1	no. 19111 collimator 2	
neutron yield	1.3 ± 15%	3.2 ± 15%	10^{13} neutrons
specific neutron fluence			
from VINIA	2.97 ± 2.8%	9.92 ± 8.1%	10^{-8} neutron/cm^2
from VINIA-NEPMC	2.77	9.80	10^{-8} neutron/cm^2
resulting neutron fluence	3.60 ± 15%	31.4 ± 15%	10^{5} neutron/cm^2
measured neutron fluence	4.73 ± 13%	43.3 ± 13%	10^{5} neutron/cm^2

For collimator 2 the correction factor 0.859 for the absorption in the glass plate of the emulsion was taken into account. It was determined from the results for collimator 1. The neutron fluences are integrated from 1 to 3 MeV. For this energy range the measured fluences are 30% and 38%, respectively, higher than those calculated. We shall discuss this together with the results for the neutron spectra.

9.2) Neutron energy spectra

Figures 9.1 and 9.2 give for both considered discharges the spectra calculated with the NEPMC software from the PTO outputs and compare them with the spectra measured for the considered discharge by the nuclear emulsion for $\Theta_{max} = 20^{\circ}$. This comparison shows that the hump on the low-energy wing of the main line around 2.45 MeV is not reproduced in the calculated spectra, as was already the case in the simulation of the measurements at the Gothenburg accelerator. We expect that this will be solved by a more carefull measurement of the dip angle of the proton tracks as well as by detailed simulation of the proton track statistics in the NEPMC software which is already under consideration.

The measured spectra are somewhat more broadened than the calculated ones. Besides the simplified treatment of track statistics the calculated line width is expected to be too small, because we neglect the gyration of fast deuterons. We checked by a test run with a constant angle between the ion velocity and flux surface that the observed order of additional broadening is also reproduced by the VINIA software when reasonable values for this angle are used.

Furthermore the results in figures 9.1 and 9.2 show that the calculated scattered background is too low. To discuss this in more detail, we compare the calculated and measured neutron fluences separately in the energy intervals between 1 and 2.1 MeV and between 2.1 and 3 MeV.

ASDEX discharge no. 16911, collimator 1,		neutron yield $1.3\times10^{13}\pm15\%$
energy range (MeV)	$1.0 \le E_n < 2.1$	$2.1 \le E_n \le 3.0$
specific neutron fluence		
from VINIA	$0.27 \pm 7.0\%$	$2.52 \pm 2.3\%$ 10^{-8} neutron/cm^2
from VINIA-NEPMC	0.36	2.41 10^{-8} neutron/cm^2
resulting neutron fluence	$0.47 \pm 17\%$	$3.13 \pm 15\%$ 10^5 neutron/cm^2
measured neutron fluence	$1.31 \pm 15\%$	$3.41 \pm 13\%$ 10^5 neutron/cm^2

ASDEX discharge no. 19111, collimator 2,		neutron yield $3.2\times10^{13}\pm15\%$
energy range (MeV)	$1.0 \le E_n < 2.1$	$2.1 \le E_n \le 3.0$
specific neutron fluence		
from VINIA	$1.28 \pm 12.6\%$	$8.64 \pm 6.5\%$ 10^{-8} neutron/cm^2
from VINIA-NEPMC	2.19	7.61 10^{-8} neutron/cm^2
resulting neutron fluence	$7.0 \pm 20\%$	$24.4 \pm 16\%$ 10^5 neutron/cm^2
measured neutron fluence	$17.8 \pm 15\%$	$25.5 \pm 13\%$ 10^5 neutron/cm^2

The broadening of the apparent neutron spectra owing to the off-axis incidence of neutrons causes a shift of neutron fluence from the higher energy interval to the lower one in the NEPMC results compared with the VINIA results.

Now for the energy range above 2.1 MeV the agreement between the two results for the fluence at the emulsion is good and well within the errorbars. In consideration of the fact that the three values involved, namely the neutron yield measured by counters, the neutron fluence per emitted neutron calculated with the VINIA-NEPMC software, and the neutron fluence measured with the nuclear emulsion, are completely independent, the agreement is exceptionally good.

Even in the investigation of neutron fluences, e.g. in calibration experiments, one of the advantages of the nuclear emulsion is its spectral resolution. It is thus only the energy range above 2.1 MeV that is of interest for comparing the numerical results with emulsion measurements for diagnostic purposes, whereas the energy range below 2.1 MeV is more of interest for investigations of the neutron scattering.

On the other hand, for the collided fluence below 2.1 MeV the measured values are about 2.7 times as large as the calculated ones but the spectra agree within one or two standard deviations of the measurements. This discrepancy is still under investigation. In principle, it may arise for four reasons:

1) from details at the port and ASDEX vessel in the parts in front of the collimators which are not taken into account in our model,
2) from underestimation of the error in the extrapolation of track number from maximum scanning angle Θ_{max} around 30^0 to 90^0,
3) from back-scattering of neutrons in the walls of the experimental hall,
4) from errors in the cross-sections for iron in the NBF files.

9.3) Decrease of neutron fluence along the emulsion axis

Owing to the decrease of the solid angle for zone 1 with increasing distance of the selected point in the emulsion we have to expect a decrease in the neutron fluence in the x-direction. This is indeed observed both experimentally and numerically.

For the standard case considered in section 7 we subdivided the area of the emulsion into four equal parts as shown in figure 9.3. In this figure the measured decrease of the neutron fluence along the x-axis (integrated over the z-direction) is given and compared with the numerical results for the four parts of the nuclear emulsion. The agreement of the observed and calculated decreases in the fluence is also very good. The difference in the absolute values corresponds to the difference in the measured and calculated neutron fluences as given above.

10) Special calculations

In order, on the one hand, to demonstrate the simplicity of considering further structural components or details of the experimental arrangement in our calculation and, on the other, to check that no essential contributions are lost, we carried out some special calculations for ASDEX discharge no. 16911 with collimator 1, taking into account

1) some parts of the divertor,
2) homogeneous material inserted between the field coils,
3) the ASDEX experimental hall.

For these orientative runs we used only 750 to 1000 emitted neutrons, and thus the error in the specific total fluence at the emulsion is 15 to 20 %.

The runs with some components of the divertor included in the ASDEX model gave no clear results; yet they demonstrate that a possible contribution from the divertor will be small. This was expected because the divertor is dominantly located in zones 2 and 3 and even the ohmic coils, which are in all zones, contribute only 2% to the total neutron fluence. Nevertheless in future we shall introduce the new ASDEX divertor in our model to make sure that its possible contributions are not lost.

The ASDEX facility is surrounded by a lot of diagnostic equipment. In order to take this into account, we filled the space between the toroidal field coils homogeneously first with 10% Al and 10% Fe and then with 50% Al and 50% Fe. Here we found no effect. This result is not surprising if it is remembered that even for collimator 2, which is mounted at one of the toroidal field coils, there was only a contribution of 0.4% from the coils to the total neutron fluence. This demonstrates again that by the adequate collimation and owing to the directional selectivity of the nuclear emulsion, the collided neutron fluence recorded is mainly produced in zone 1 of the collimator.

The run with the ASDEX hall around the facility tends to give higher values for the collided fluence, but the effect is still within the errorbars and needs further investigation.

Including the ASDEX hall in our model, we are also able to calculate the spectral neutron fluence in the control room. We considered the area shown in figure 3.6 and calculated there a mean specific neutron fluence of 0.49×10^{-11} neutrons/cm^2 per emitted neutron. This is a factor of 2.8×10^4 less than the fluence at the position of collimator 1 inside the hall. The spectrum for the

fluence in the control room is shown in figure 10.1 and compared with the spectral fluence at the position of collimator 1. The low-energy part is strongly suppressed again owing to the energy dependence of the cross-sections. The investigation of the angular dependence of the spectral neutron fluence outside the ASDEX hall may be an interesting future application of our work.

11) Final remarks

The work reported here constitutes a bench mark of the VINIA-NEPMC software against nuclear emulsion measurements. The results are very encouraging and justify continuation of the work.

The structure of our software package offers several advantages. Firstly, the four main parts, namely the plasma neutron source, the tokamak structure, the migration of neutrons, and the response of the detector are independend and can be improved stepwise corresponding to the progress of the investigations as well as exchanged to allow for a treatment of other problems like i.e. special neutron production mechanisms or other detectors. Secondly, it combines the treatment of the detailed structure and energy spectrum of the neutron source with a fine energy mesh calculation of neutron migration and the special response of the detector. Thus, for the first time, we are able to investigate the effects of neutron scattering and source extent on the detected neutron signal.

To investigate and possibly remove the remaining differences between the calculated and measured neutron fluences and spectra, the following investigations and improvements seem to be necessary.

1) The statistical treatment in the NEPMC software of the proton tracks and their measurement has to be improved and checked against better measurements at an accelerator. This work has been initiated.

2) Next, including some improvements in track scanning now being prepared, we have to use a nuclear emulsion measurement from ASDEX with a higher track density to reduce the statistical error in the spectra.

3) In the standard VINIA calculations the divertor and the ASDEX hall are to be included.

4) In the VINIA calculation in the future the more updated EFF-1 data file has to be used instead of the ENDF/B-4 file.

5) Taking into account the ion gyration and its effect on the emitted neutron spectrum is a more serious problem. There seems to be a possibility of extracting the relevant data from FREYA code calculations. Preparations are already being made to improve the calculation of the angle dependence of the emitted neutron energy spectrum by taking into account the thermal distribution of the background plasma.

Concerning further applications, the NEPMC software has now been adapted to handle also collimators with an arbitraty direction of their axis allowing calculations for collimators viewing the plasma from an arbitrary position and any direction.

The γ-production during the migration of neutrons through the ASDEX device was not considered in this work though it is known from the nuclear reactions in the VINIA calculations, because it is of no interest for nuclear emulsion measurements. It may be a further application in simulating of other diagnostics to treat also the migration of this γ-radiation and the X-radiation emitted from the plasma.

References

[1] K.Hübner, R.Bätzner, H.Hinsch, R.Rapp, H.Wurz, A.Eberhagen, O.Gehre, V.Mertens, ASDEX Team, Neutral Injection Team,
"Neutron Production during Deuterium Injection in Deuterium Plasmas in ASDEX"
12th Europ. Conf. on Controlled Fusion and Plasma Physics, Budapest 1985, part 1, pp 231-234

[2] J.S.Brzosko, B.V.Robouch, L.Ingrosso,
"Openings in a Fusion Reactor Blanket (Tokamak Type) - Trends in Nuclear Charectaristics"
IEEE Transactions in Plasma Science, Vol.PS-15, (1987) pp 16-27

A short description of the results of this report is published in

[3] B.V.Robouch, K.Hübner, R.Bätzner, M.Roos, L.Ingrosso, H.Rapp, H.Wurz, ASDEX Team
"VINIA and NEPMC Code Numerical Evaluation of Neutron Scattering for Neutron Diagnostics on ASDEX"
14th Europ. Conf. on Controlled Fusion and Plasma Physics, Madrid 1987 part 3, pp 1298-1301

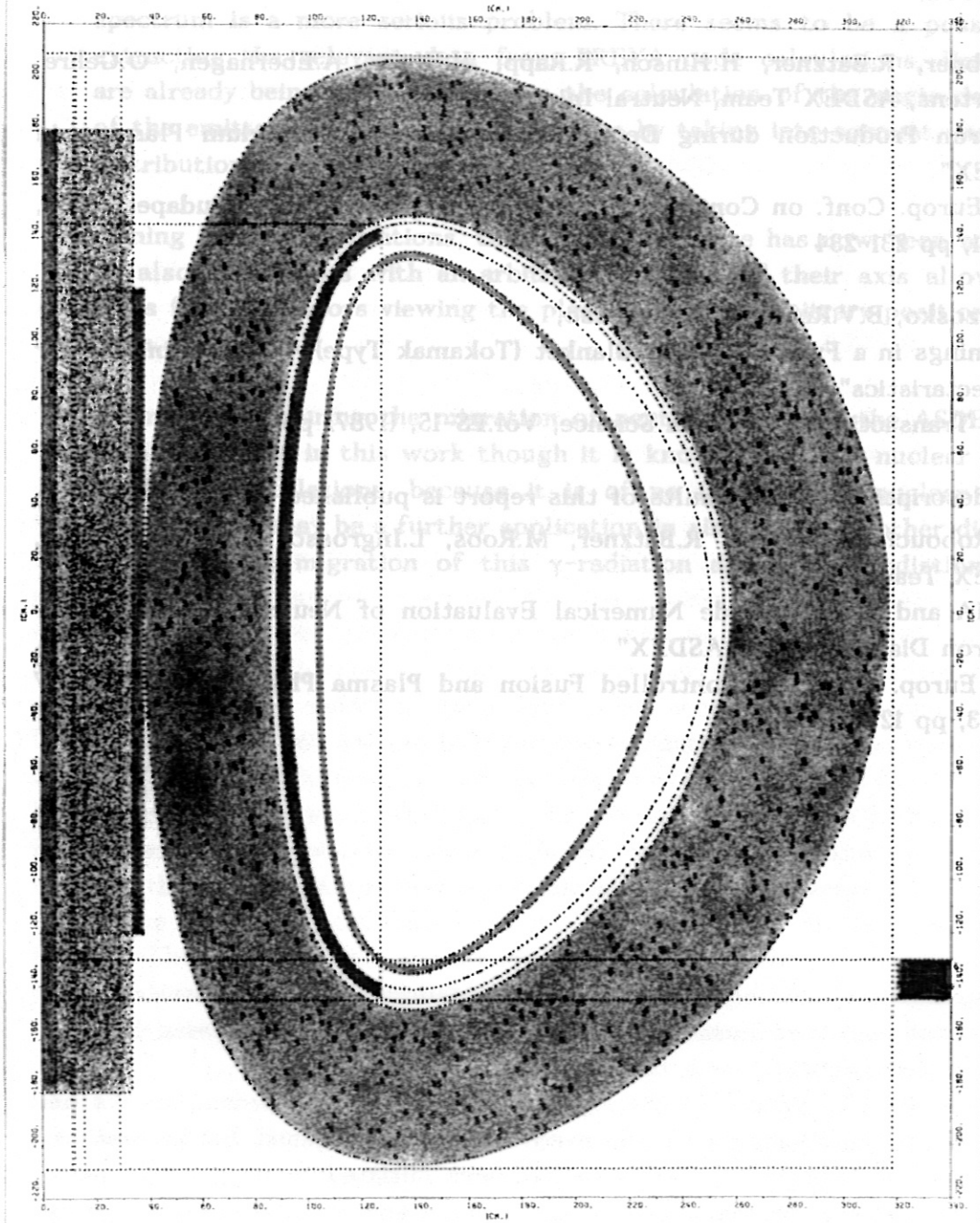

Fig. 3.1: ASDEX model used in the VINIA calculations, vertical-axial cross-section through a toroidal field coil

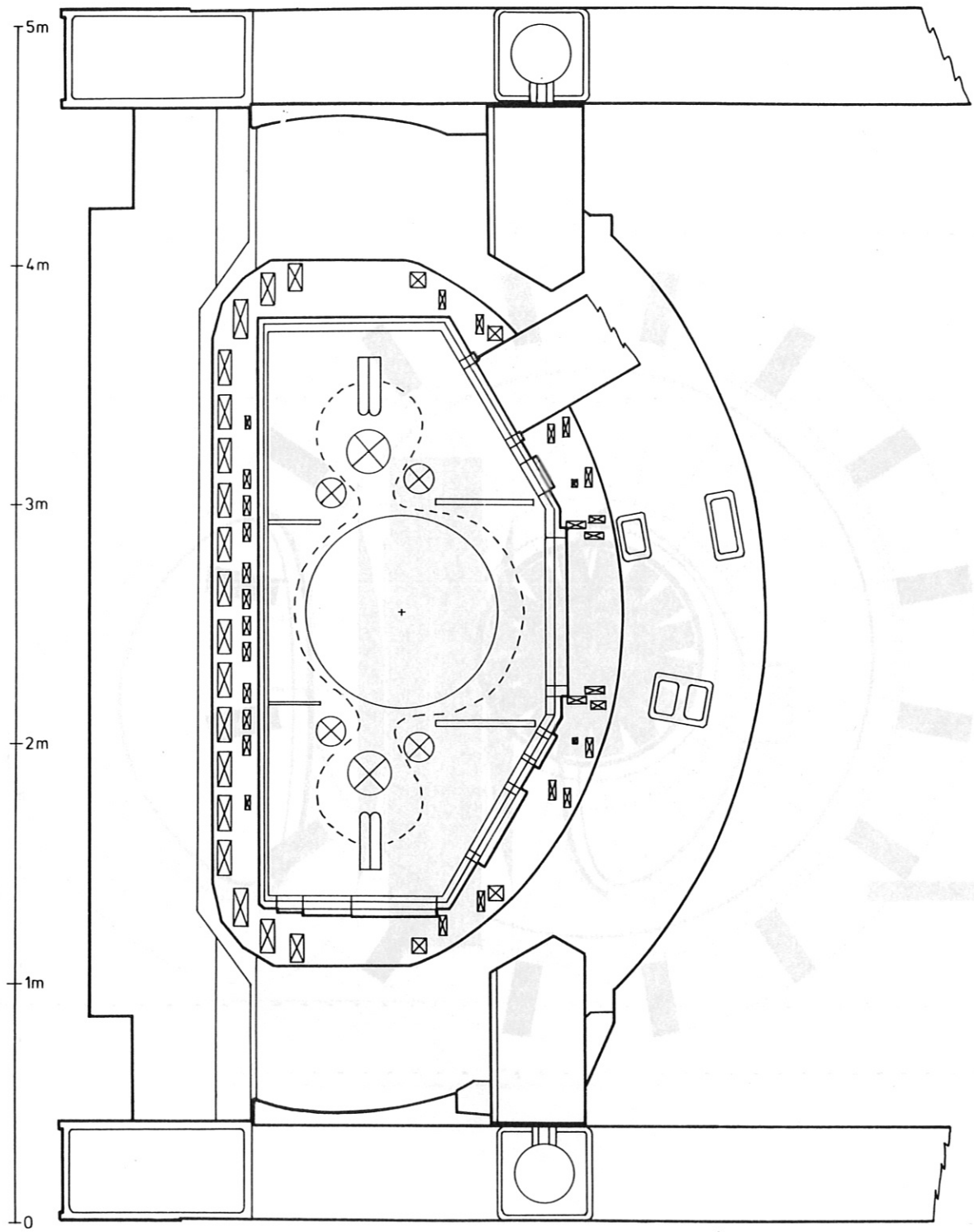

Fig. 3.2: Cross-section of real ASDEX toroidal field coils

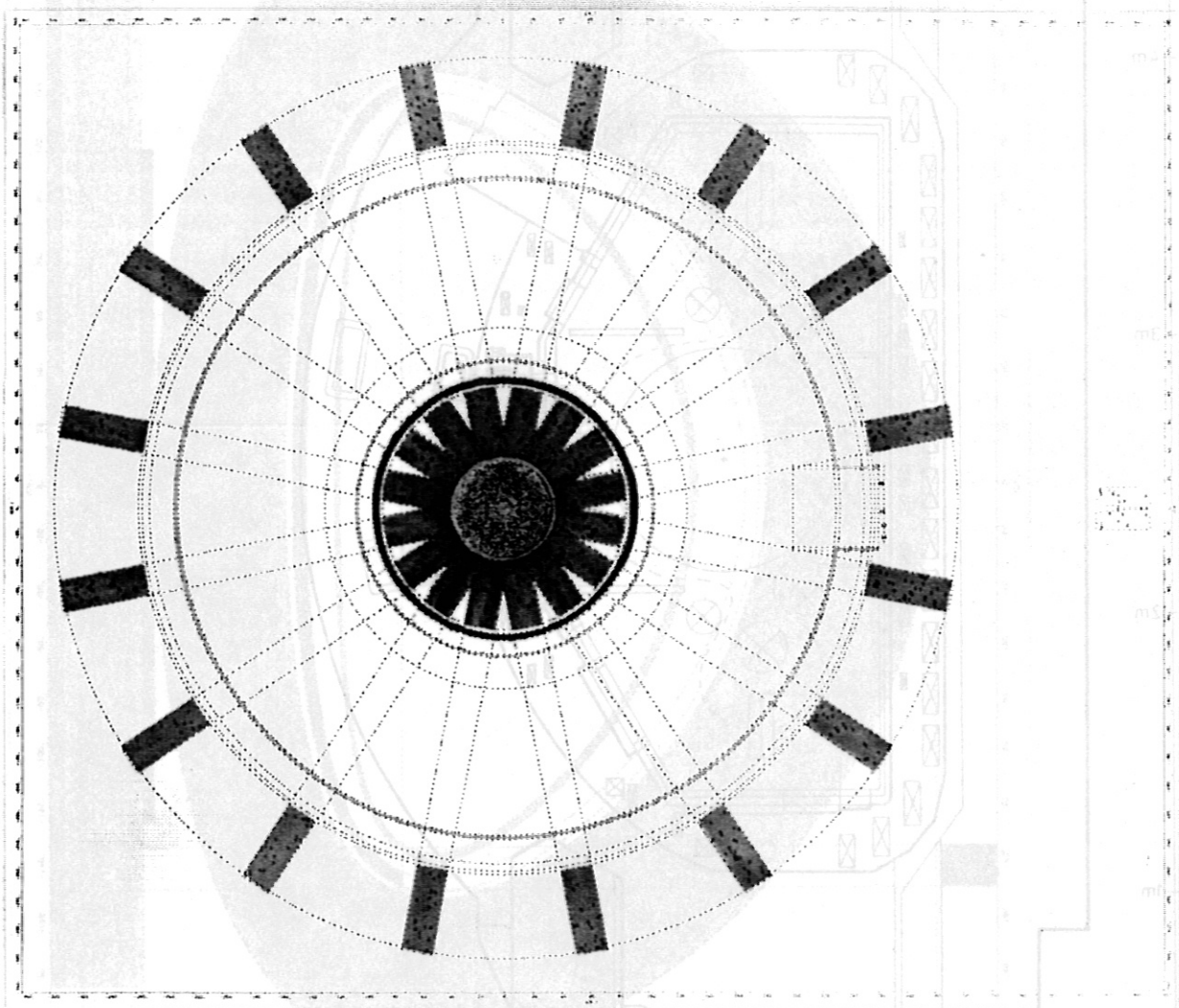

Fig. 3.3: ASDEX model used in the VINIA calculations, horizontal-equatorial cross-section (x-y plane)

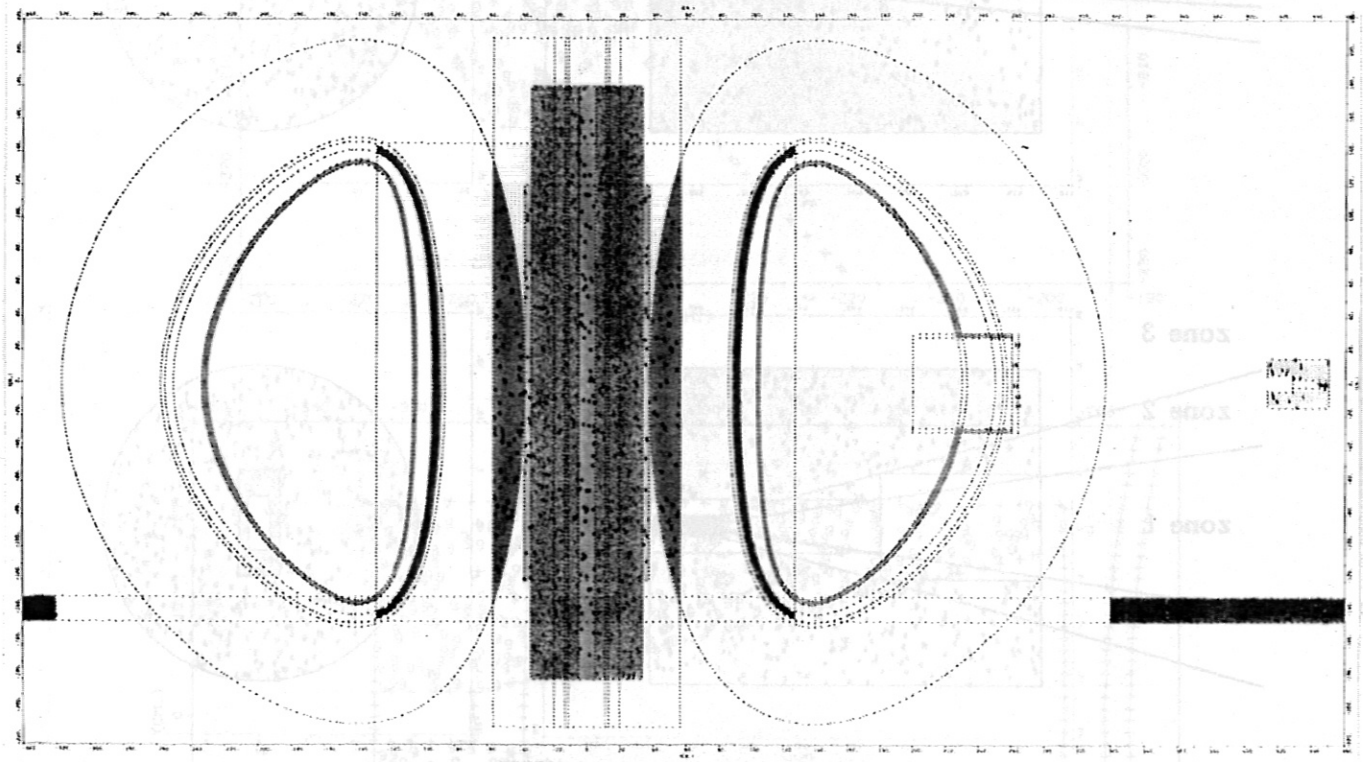

Fig. 3.4: ASDEX model used in the VINIA calculations, vertical-axial cross-section (x-y plane) through the centre of the nuclear emulsion

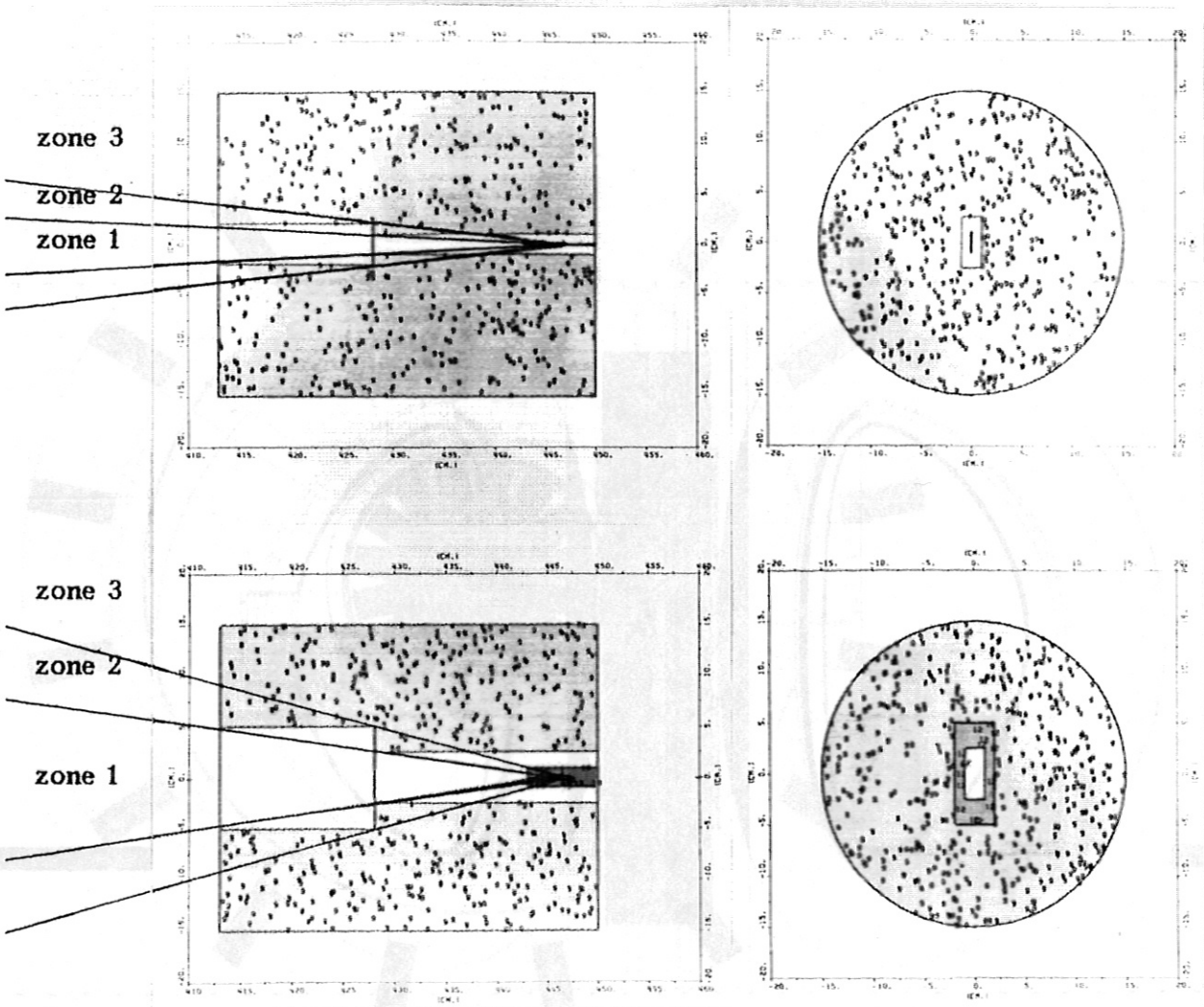

Fig. 3.5: Horizontal and vertical cross-sections through the collimator 1 to illustrate the three different zones

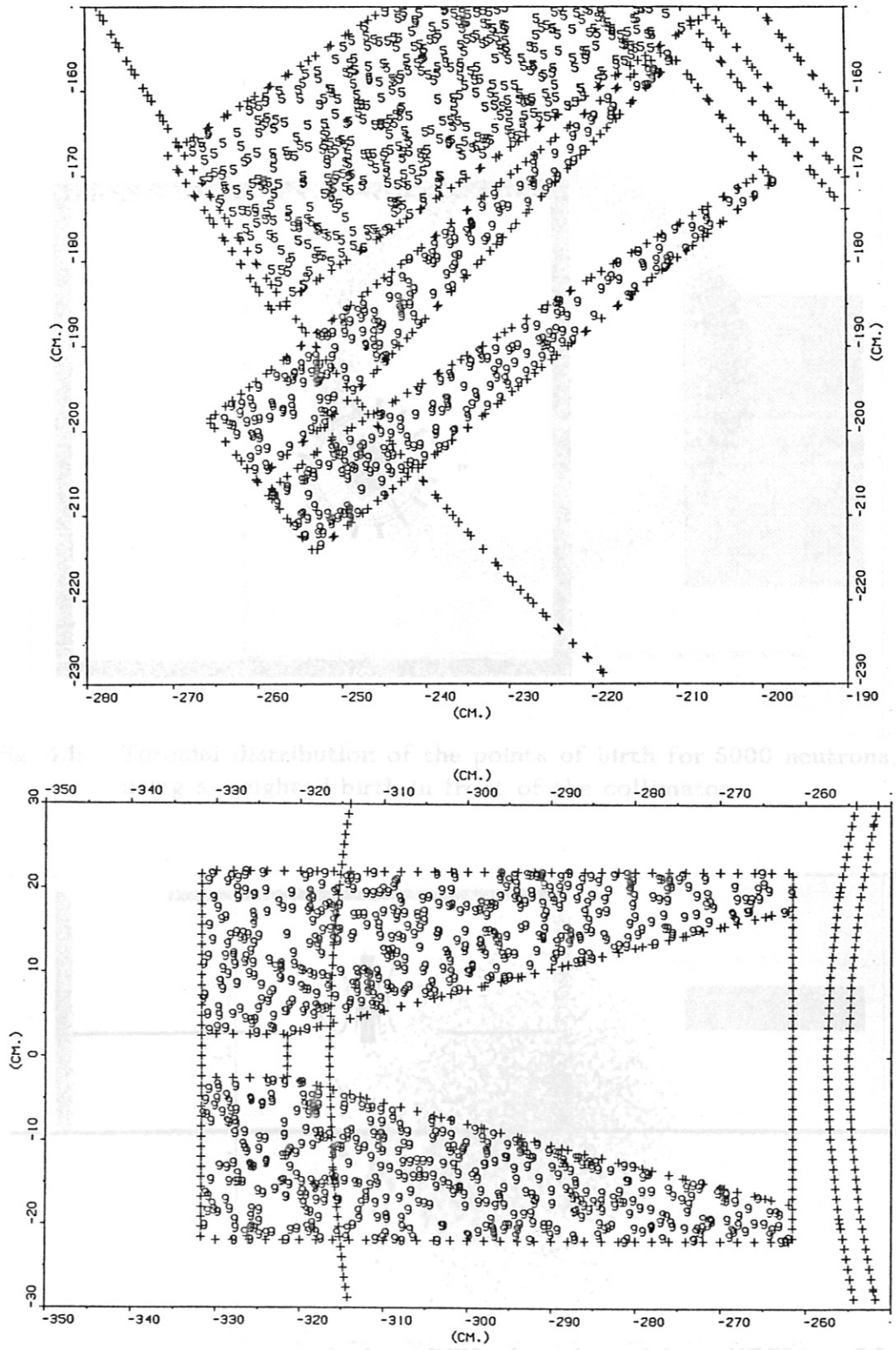

Fig. 3.6: Horizontal and vertical cross-sections through the collimator 2

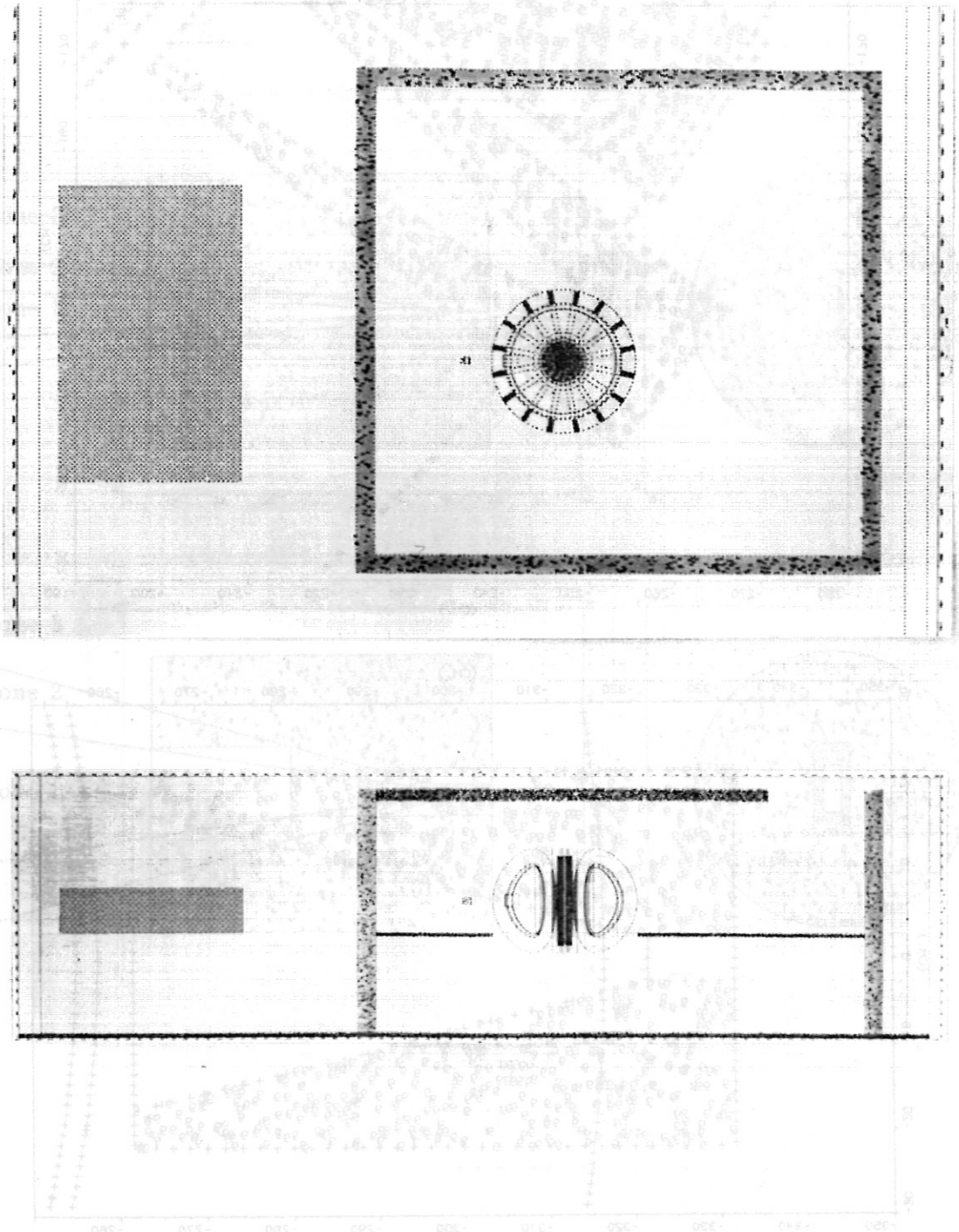

Fig. 3.7: ASDEX model used in the VINIA calculations,
ASDEX facility with torus hall and control room,
a) horizontal cut, b) axial-vertical cut in east-west direction

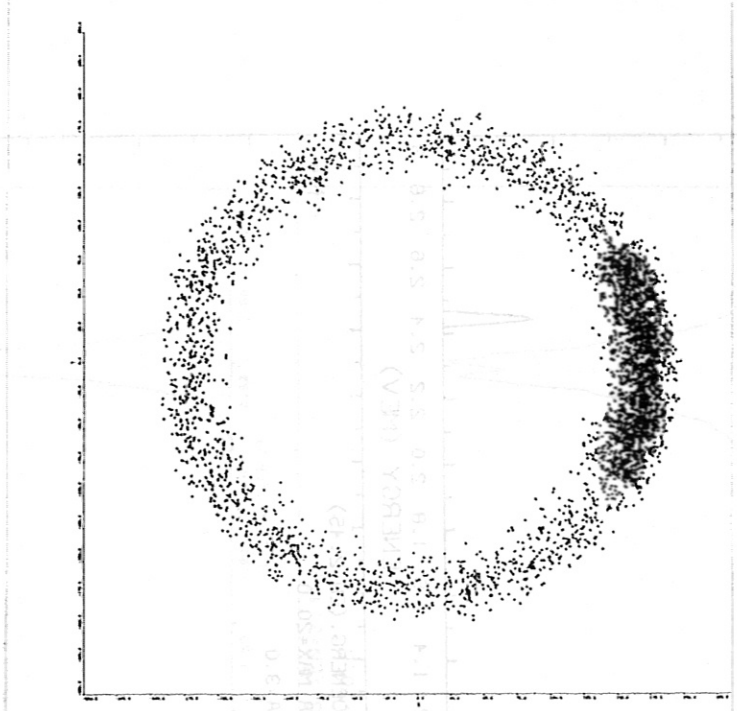

Fig. 4.1: **Toroidal distribution of the points of birth for 5000 neutrons, using a weighted birth in front of the collimator**

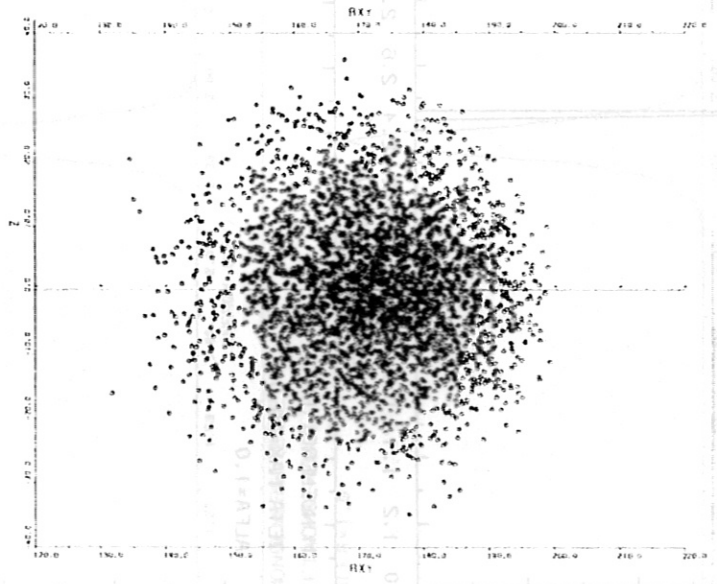

Fig. 4.2: **Poloidal distribution of the points of birth**

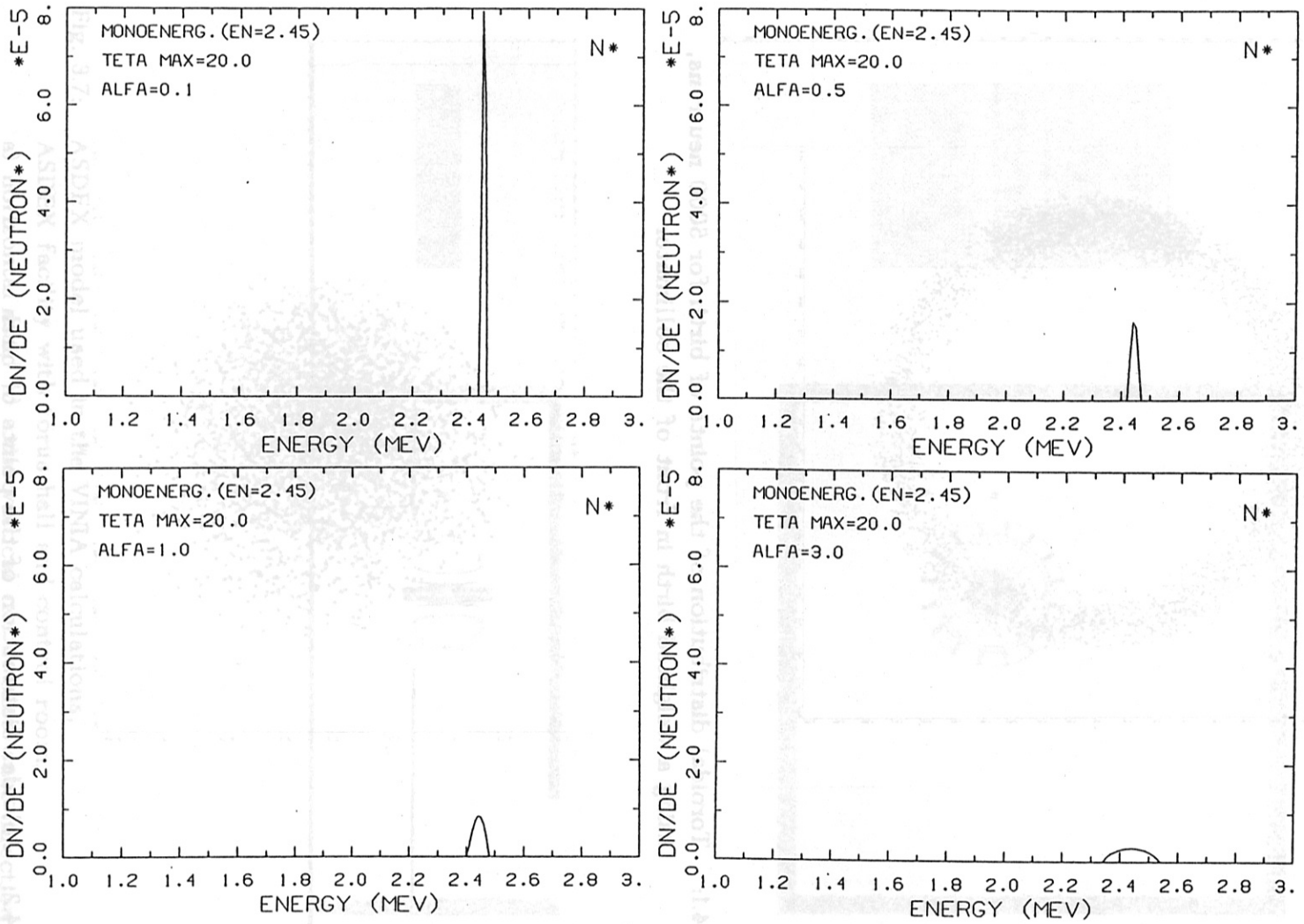

Fig. 5.1: Response function of the nuclear emulsion for an off-axis mono-energetic point source

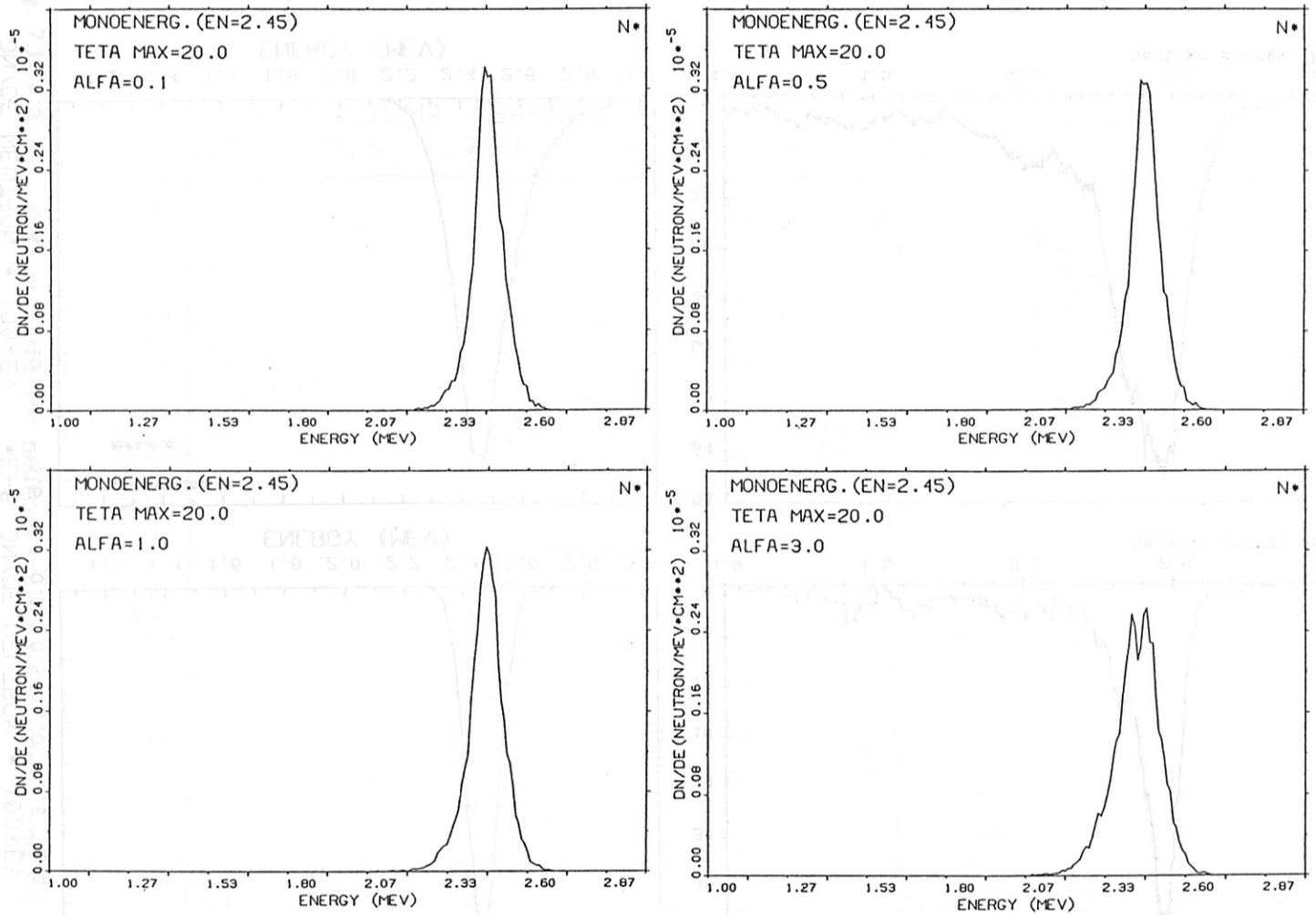

Fig. 5.2 : Response function of the nuclear emulsion for an off-axis mono-energetic point source, including proton track statistics and errors of track measurements

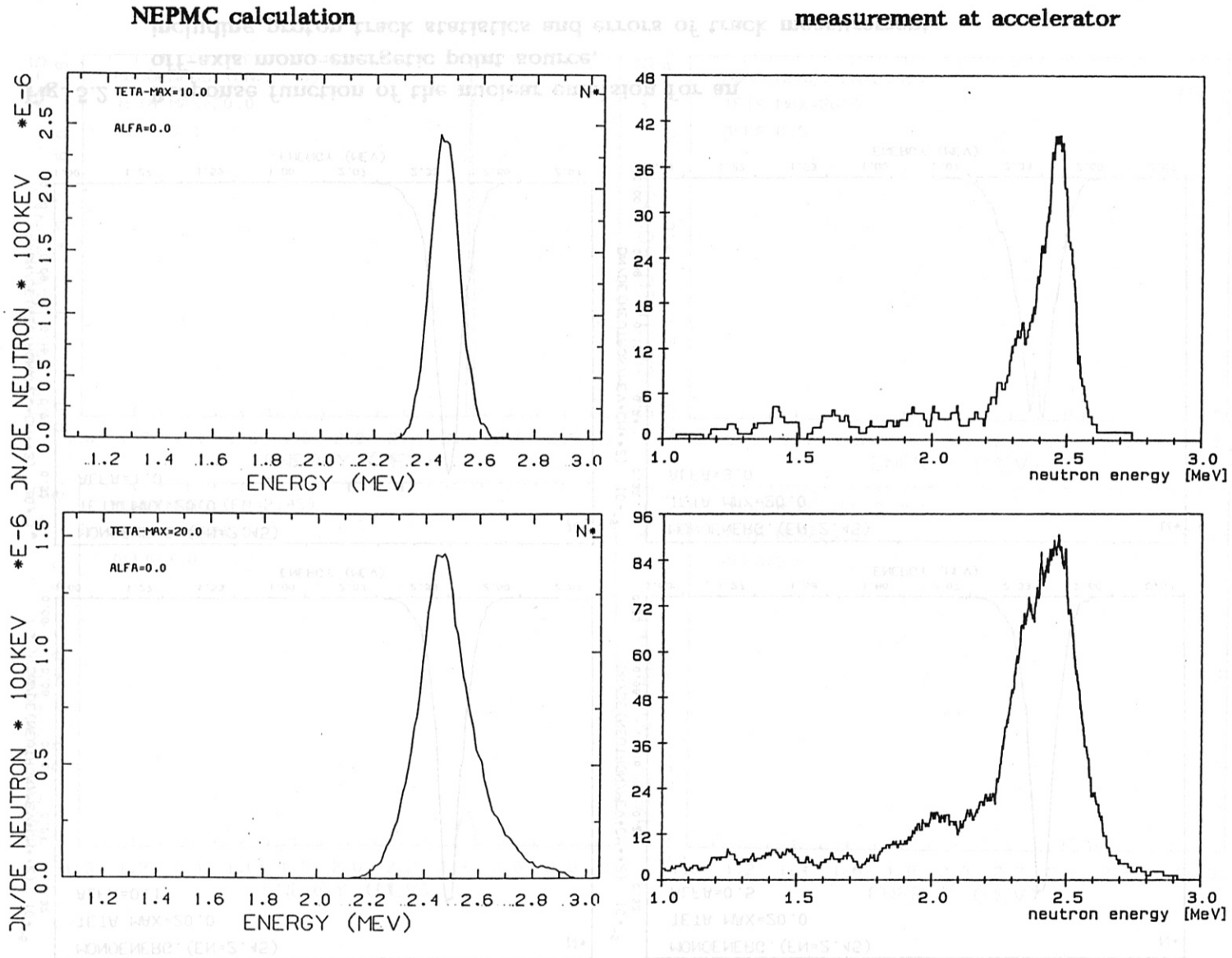

Fig. 5.3: Response function of the nuclear emulsion calculated with the NEPMC software compared to measurements at the Gothenburg accelerator

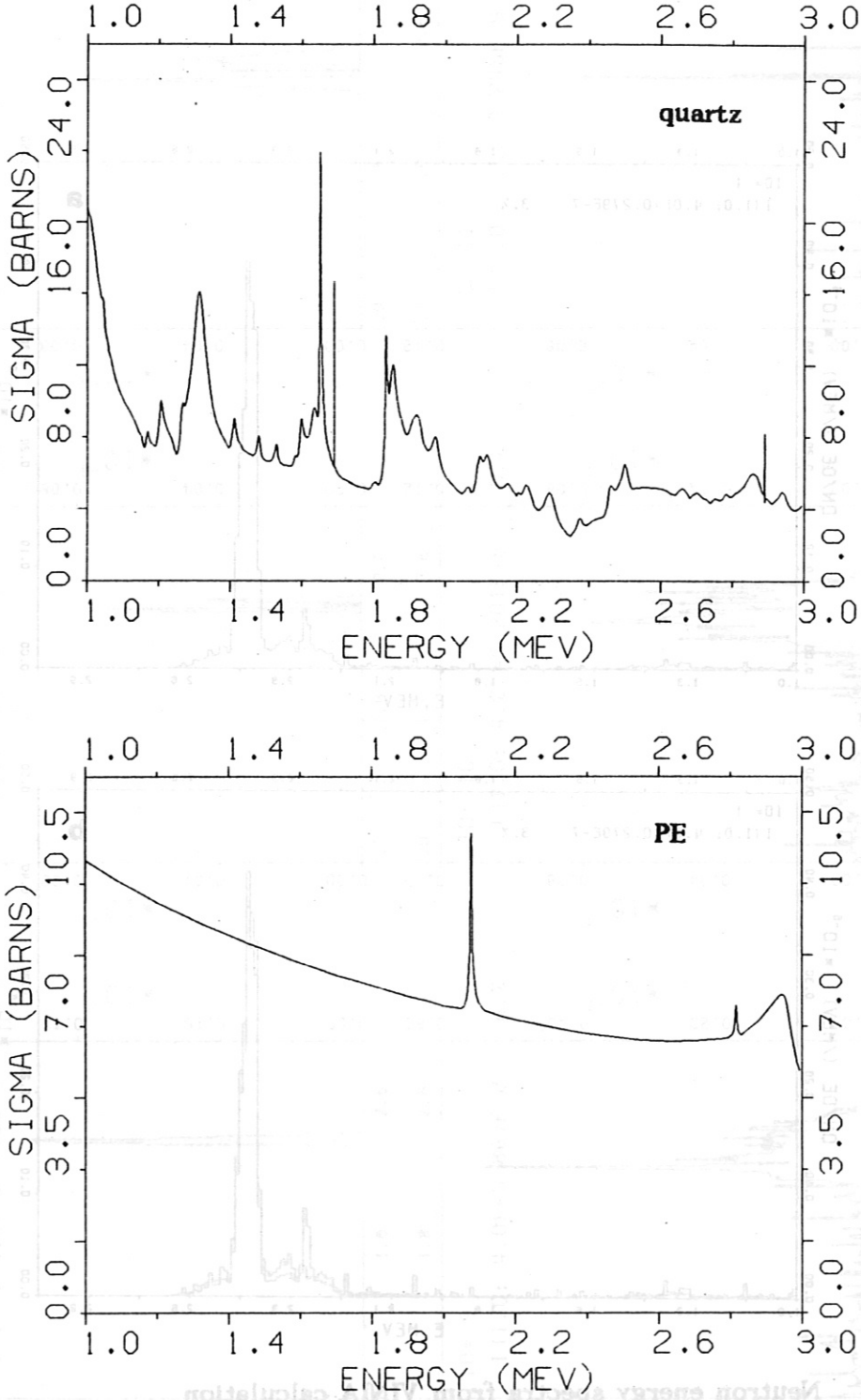

Fig. 7.1: Total cross-sections for neutron collisions in quartz and PE

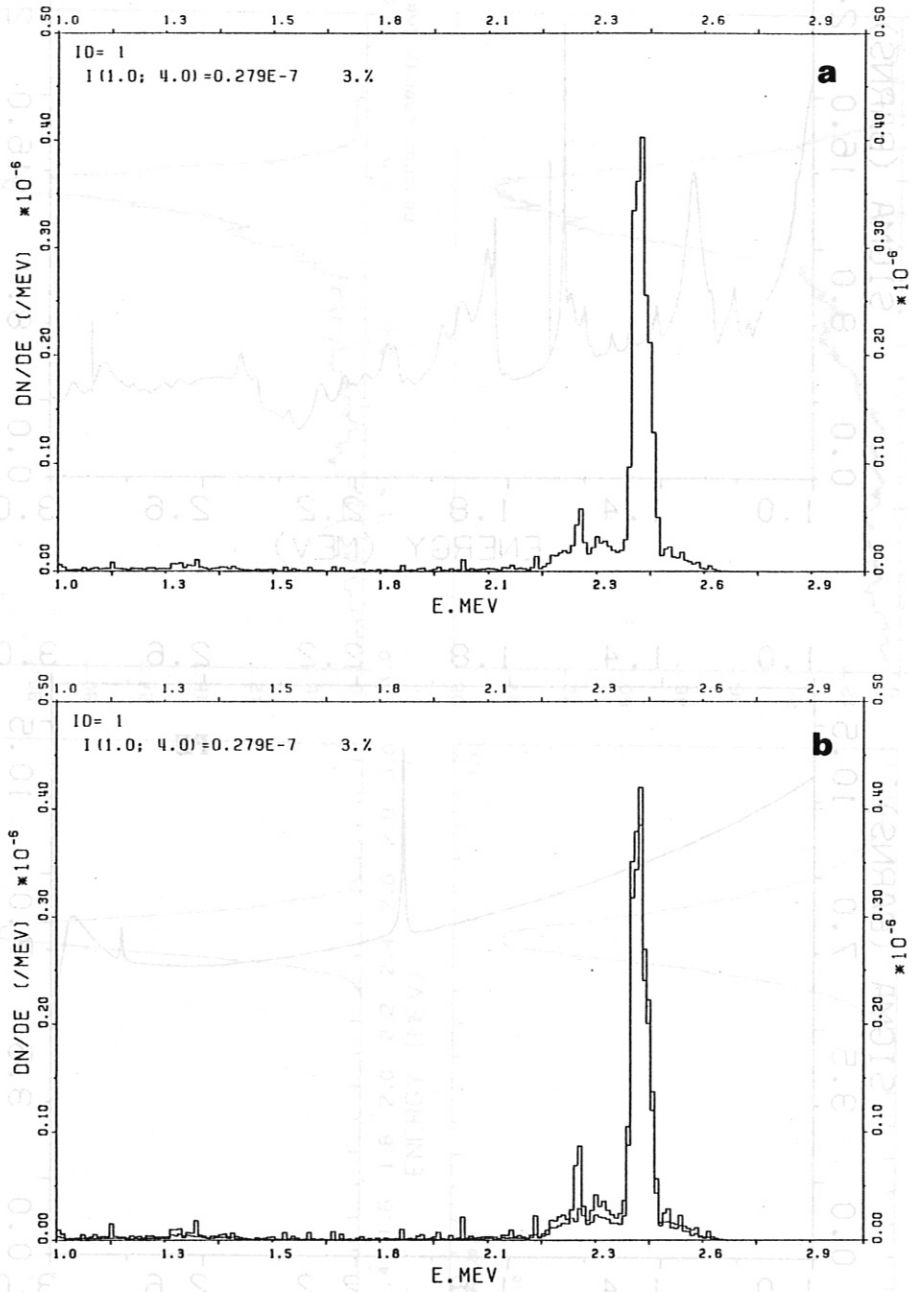

Fig. 7.2: **Neutron energy spectra from VINIA calculation for ASDEX discharge no. 16911 with collimator 1, a) total fluence per emitted neutron b) standard deviation for spectrum (a)**

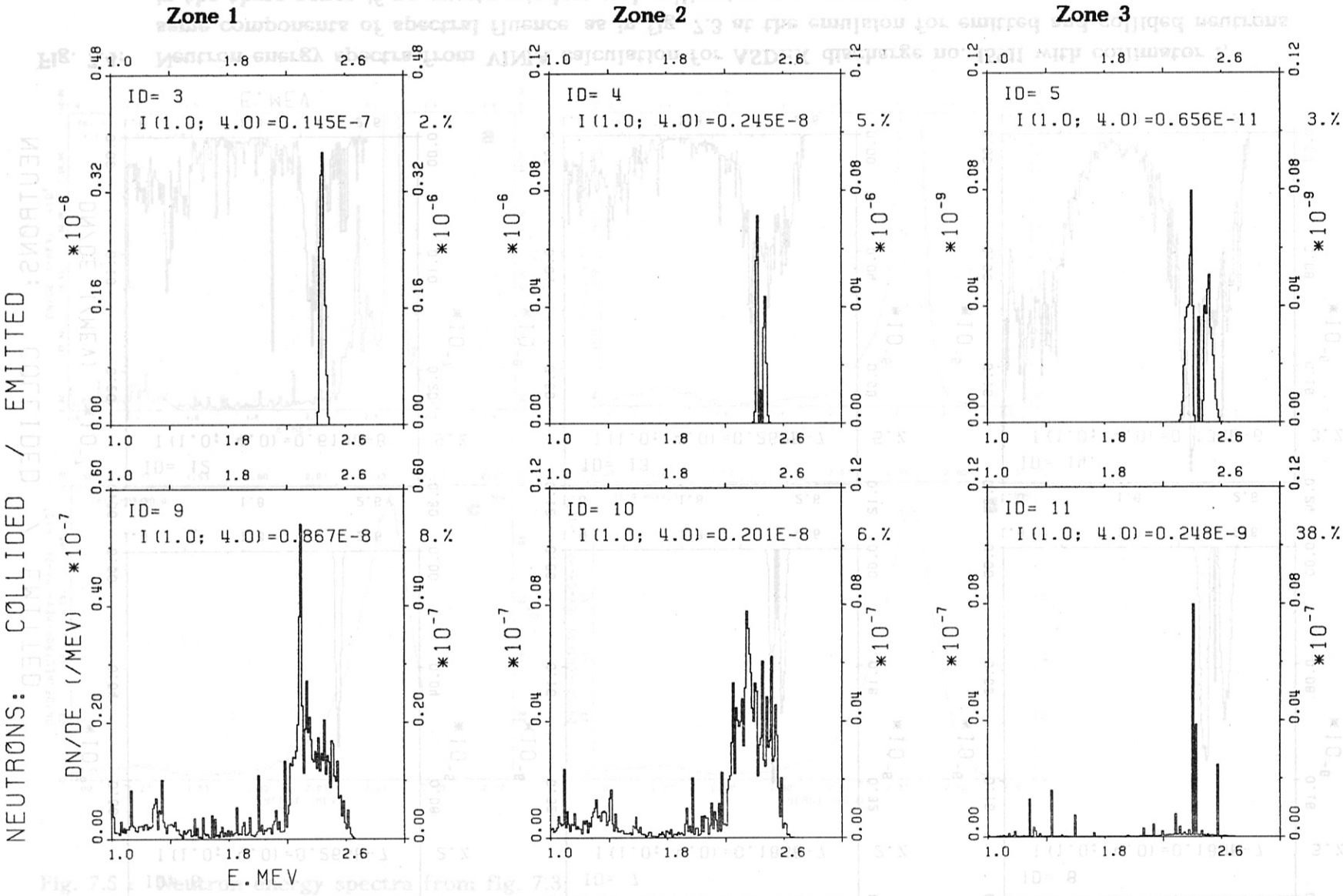

Fig. 7.3: Neutron energy spectra from VINIA calculation for ASDEX discharge no. 16911 with collimator 1, components of spectral fluence at the emulsion for emitted and collided neutrons in the three zones

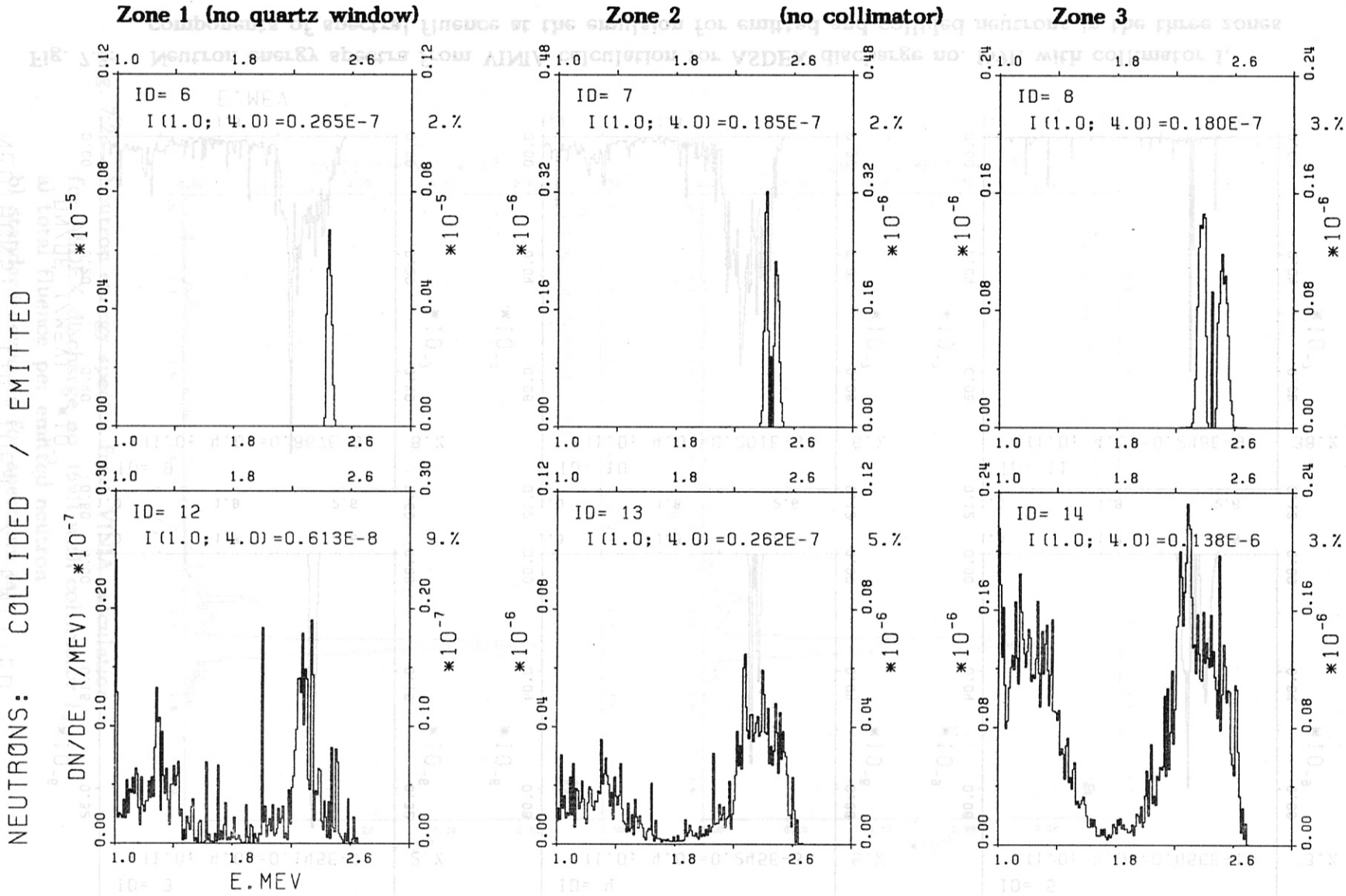

Fig. 7.4: **Neutron energy spectra from VINIA calculation for ASDEX discharge no. 16911 with collimator 1, same components of spectral fluence as in fig. 7.3 at the emulsion for emitted and collided neutrons in the three zones if no quartz window and collimator were present**

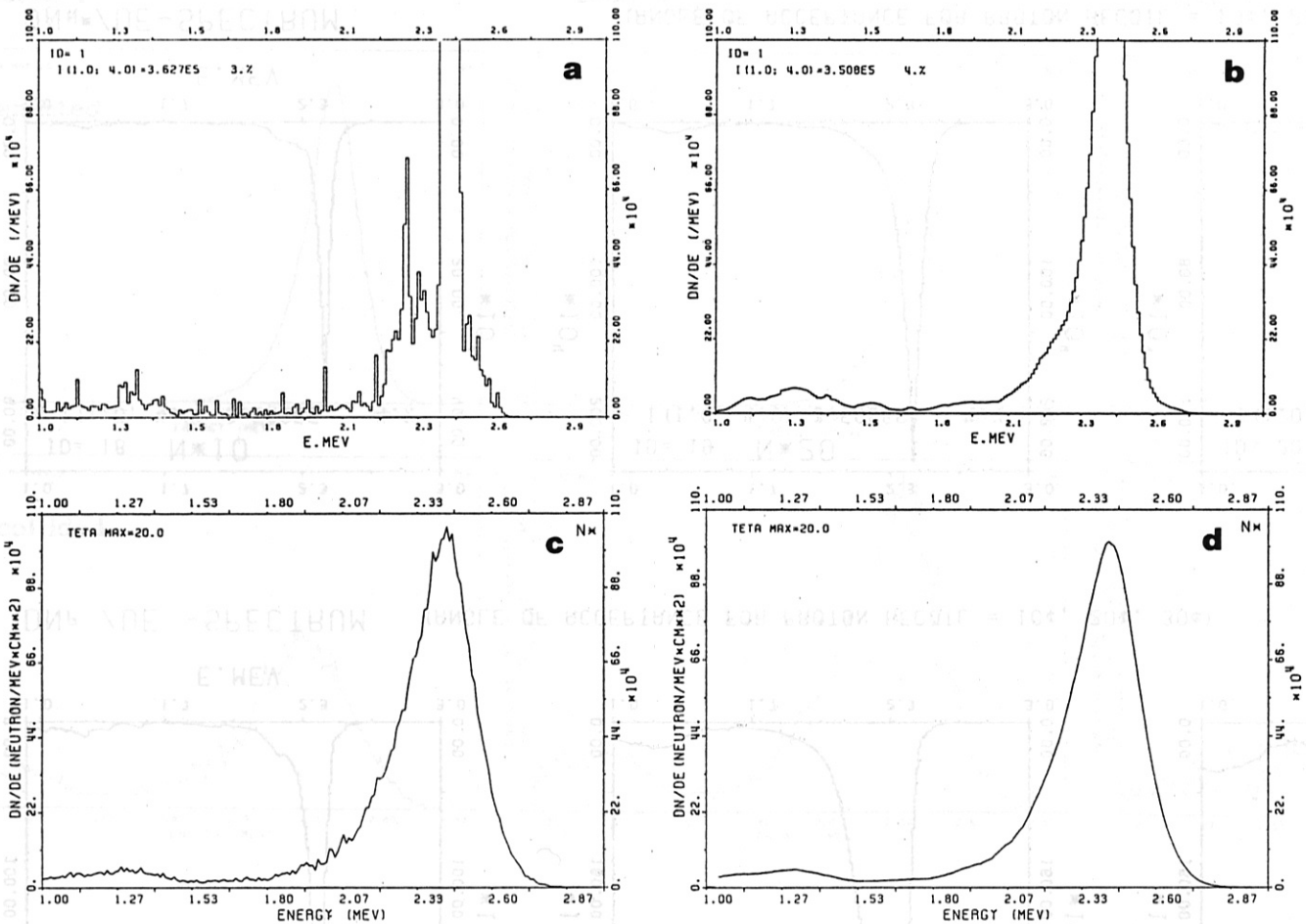

Fig. 7.5 : Neutron energy spectra from fig. 7.3,
a) VINIA calculation, b) NEP calculation, c) NEPMC calculation,
d) NEPMC calculation, smoothed over 100 keV intervalls

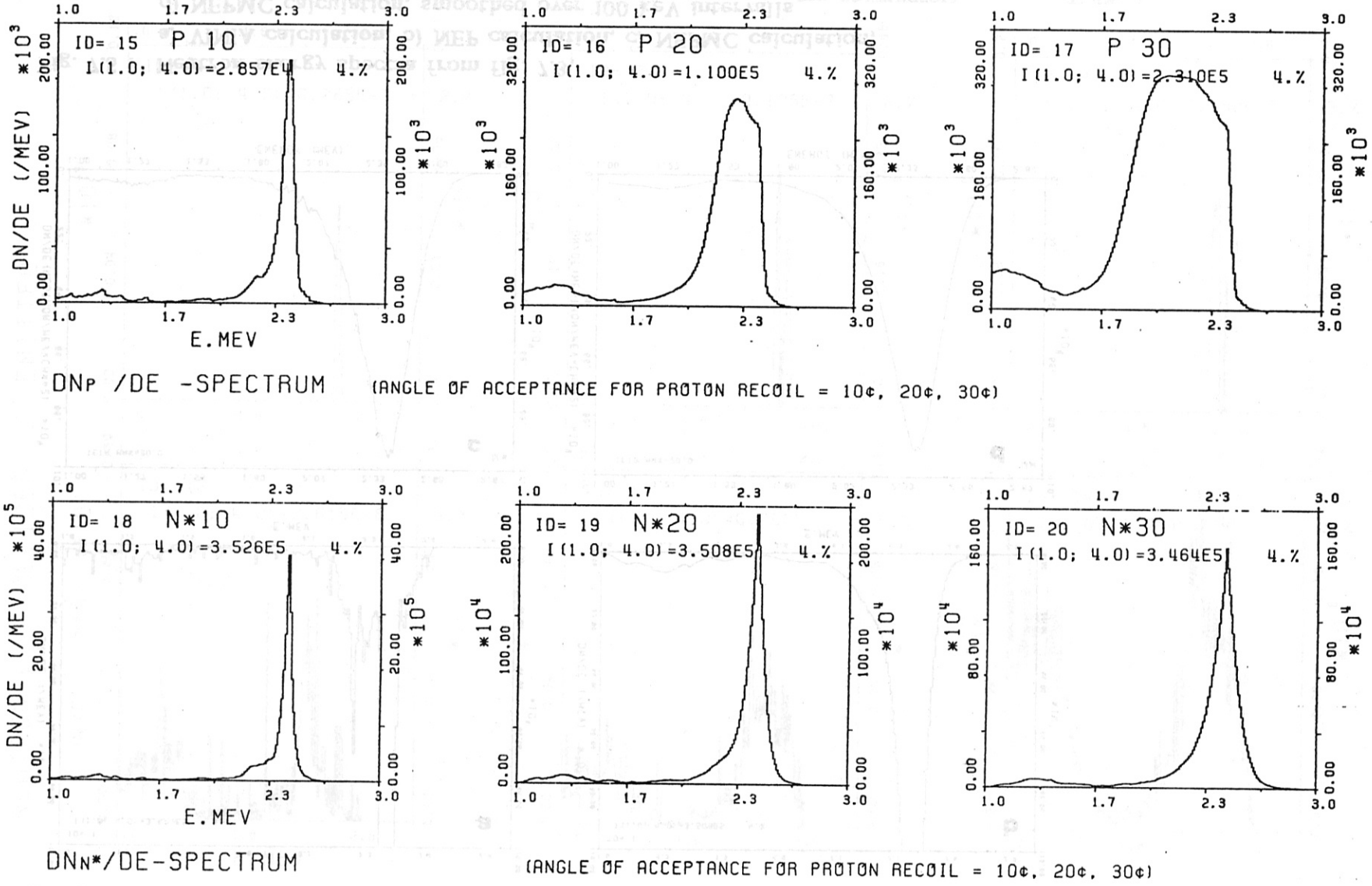

Fig. 7.6: **Proton and neutron energy spectra for ASDEX discharge no. 16911 with collimator 1 calculated by NEP software using VINIA results**

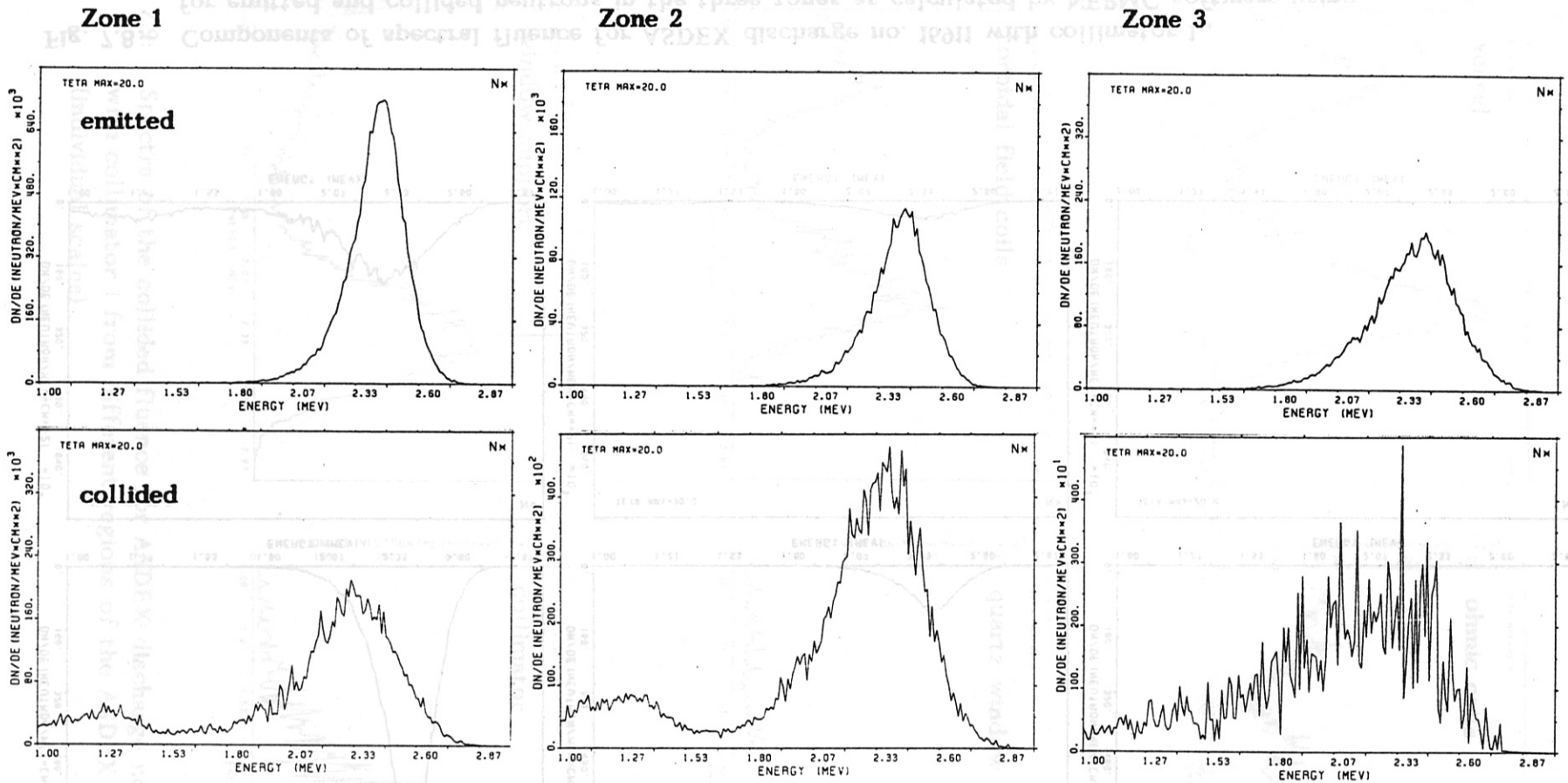

Fig. 7.7: Components of spectral fluence for ASDEX discharge no. 16911 with collimator 1, for emitted and collided neutrons in the three zones as calculated by NEPMC software using VINIA results

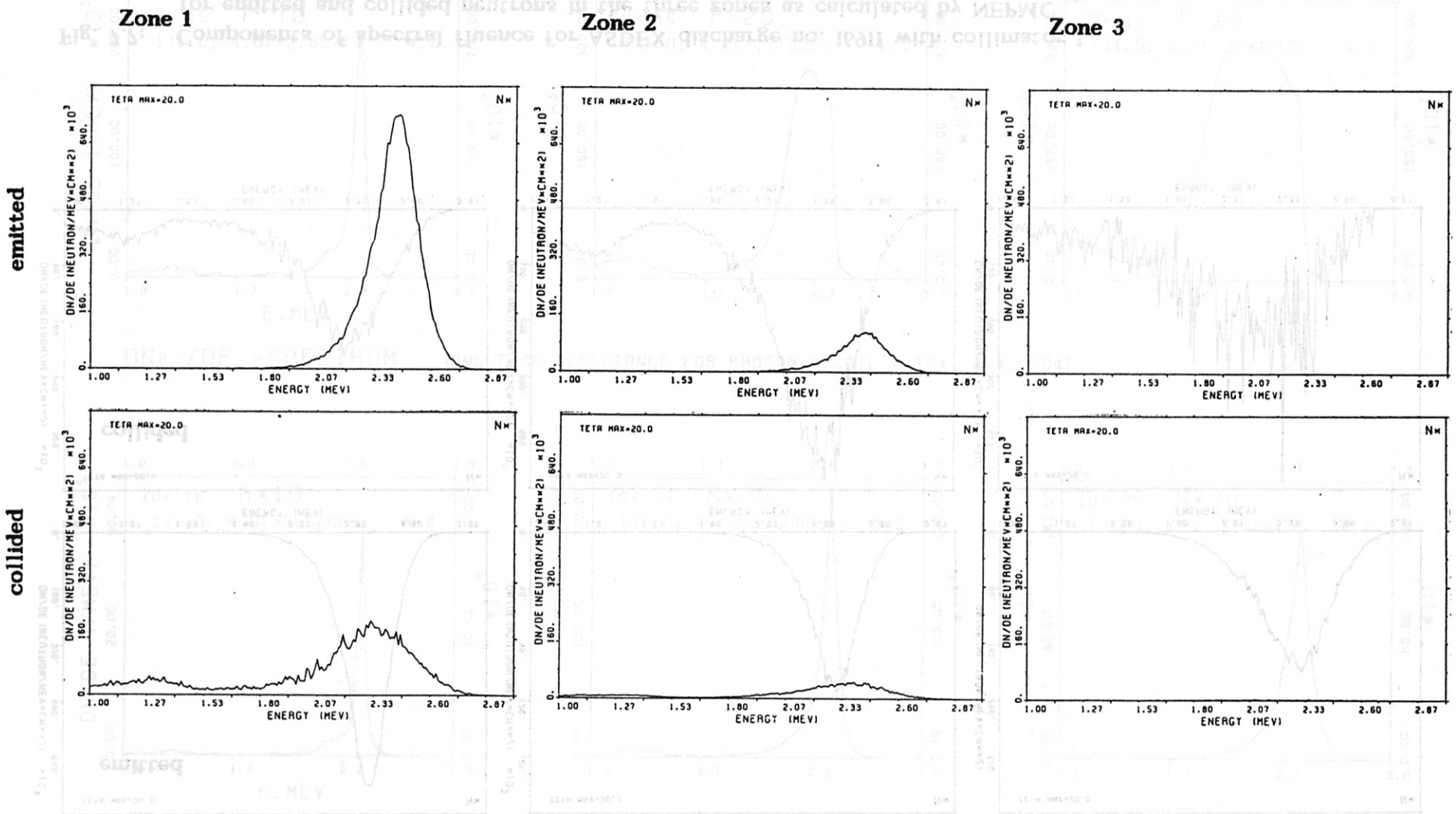

Fig. 7.8: Components of spectral fluence for ASDEX discharge no. 16911 with collimator 1, for emitted and collided neutrons in the three zones as calculated by NEPMC software using VINIA results as in fig. 7.6 but plotted with the same scale ($8 \cdot 10^4$ neutron/MeV·cm^2 per division)

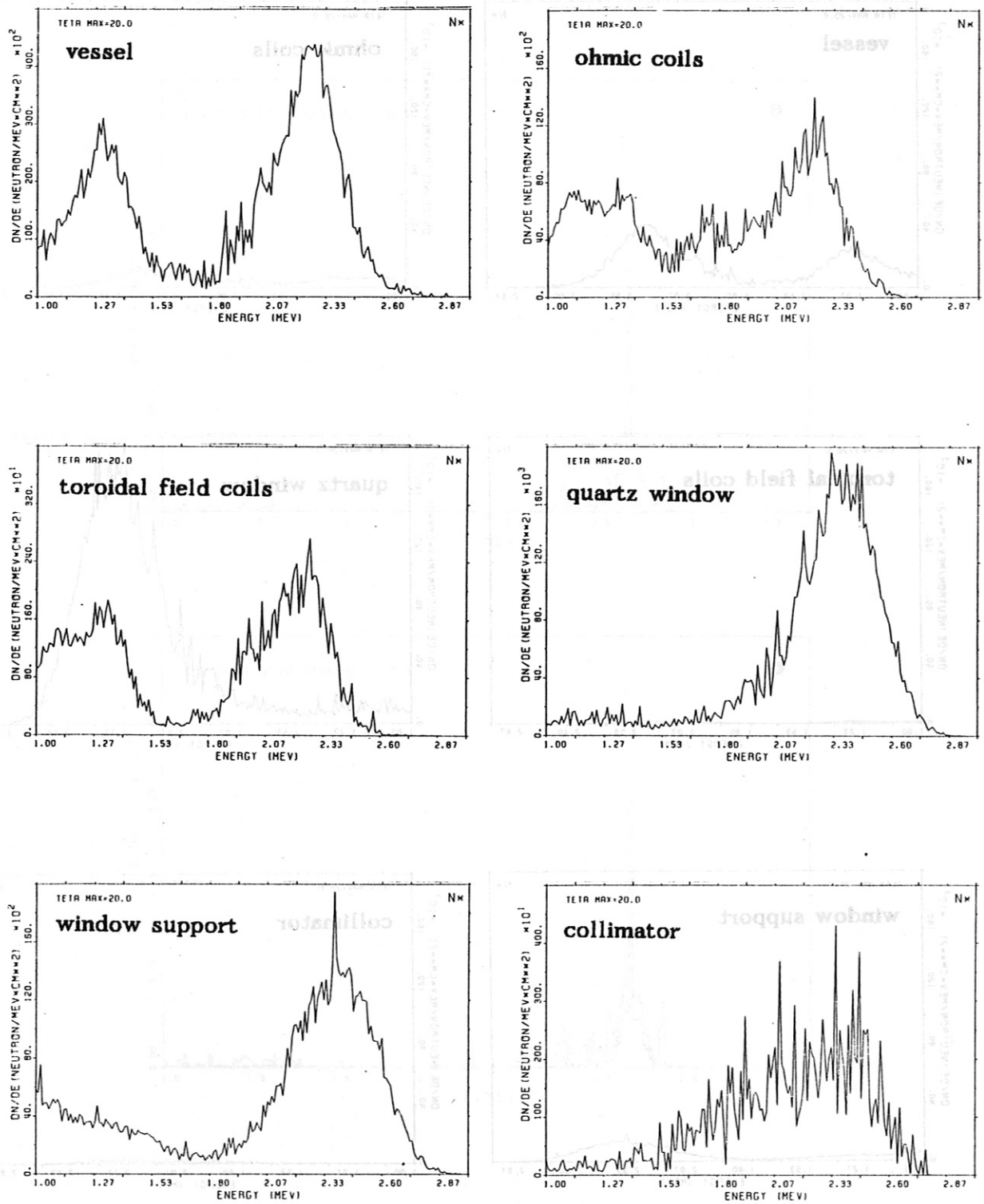

Fig. 7.9: Spectra of the collided fluence for ASDEX discharge no. 16911 with collimator 1 from different regions of the ASDEX device (individual scales)

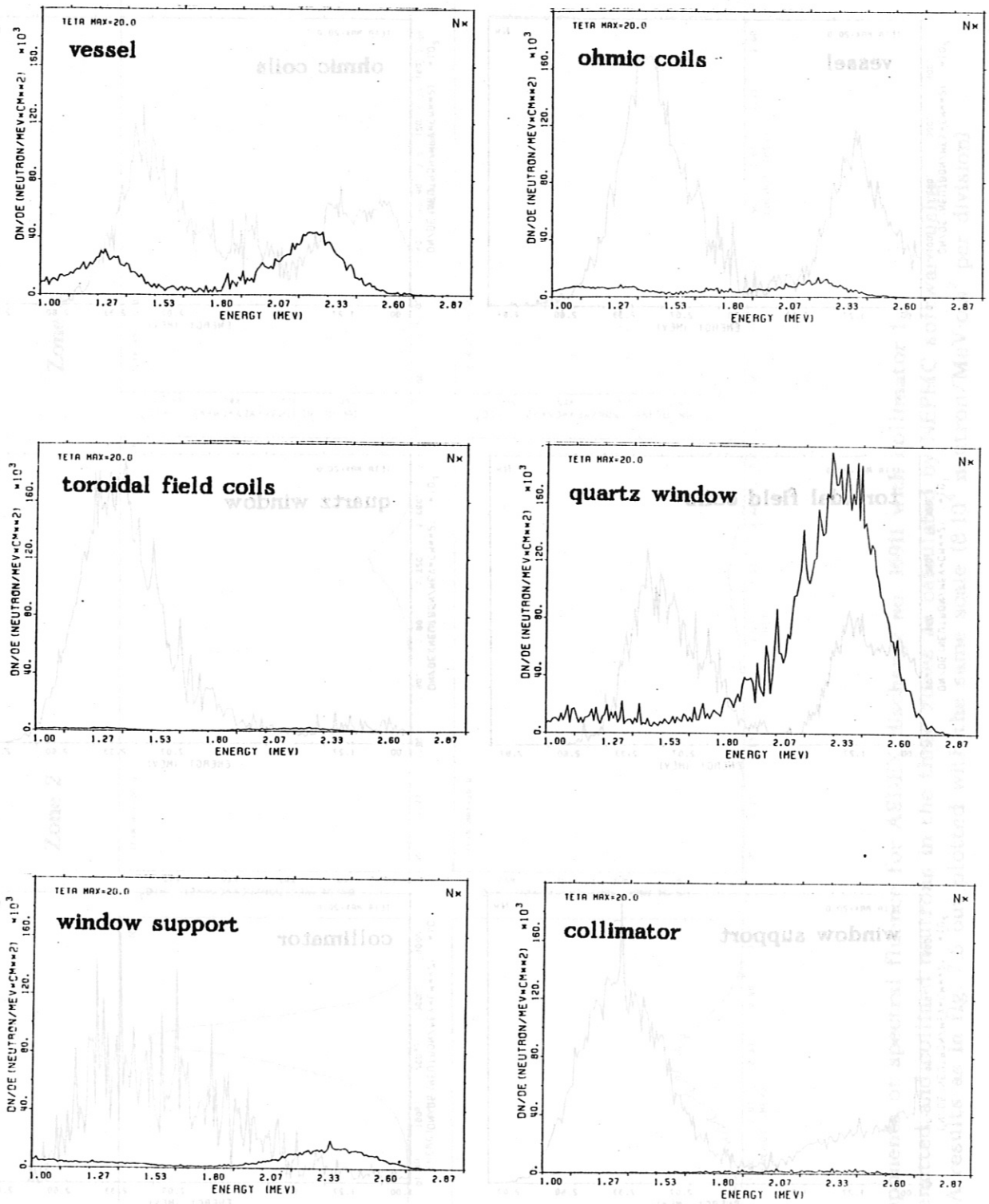

Fig. 7.10: Spectra of the collided fluence for ASDEX discharge no. 16911 with collimator 1 from different regions of the ASDEX device (identical scales)

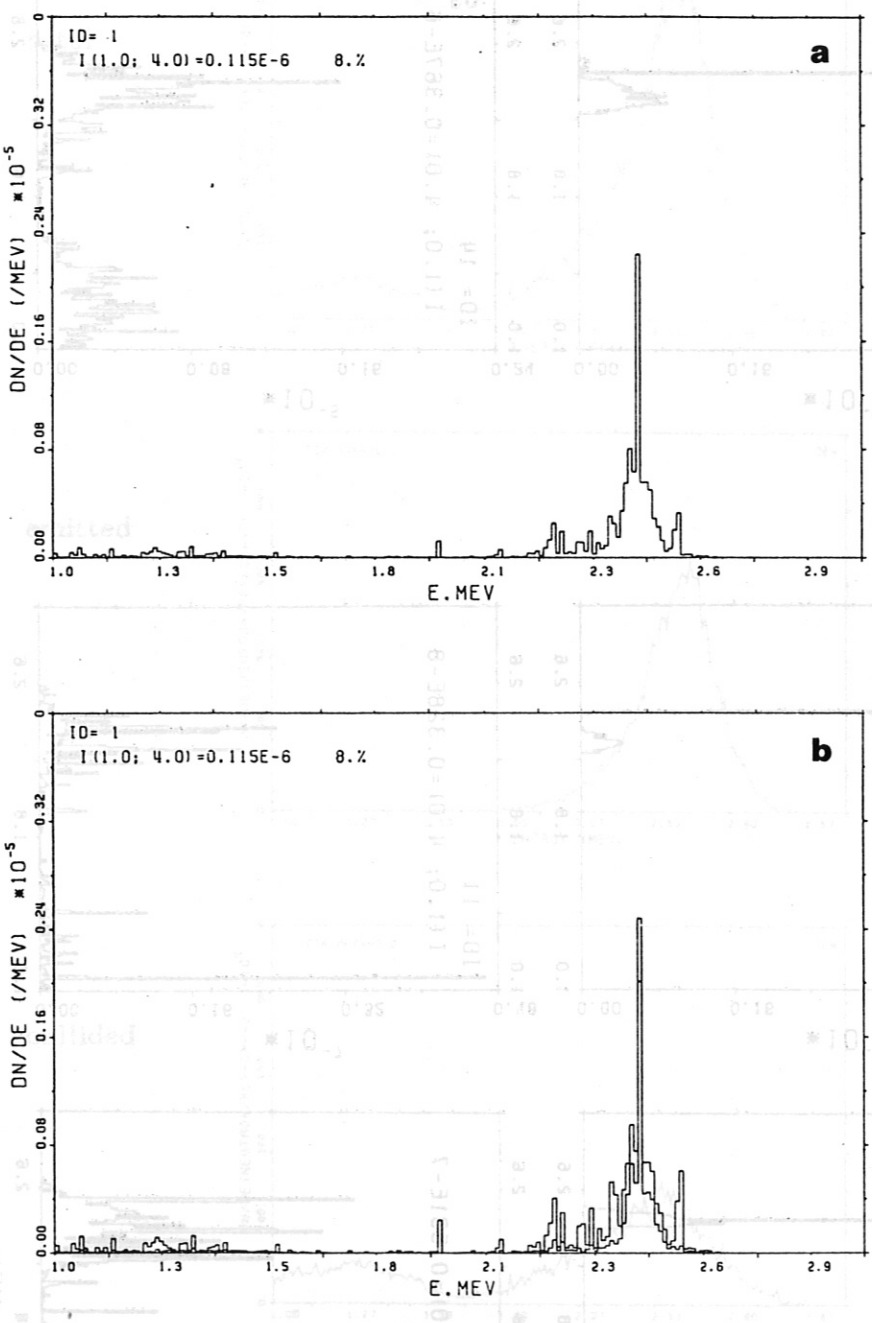

Fig. 8.1: **Neutron energy spectra from VINIA calculation for ASDEX discharge no. 19111 with collimator 2,**
a) total fluence per emitted neutron
b) standard deviation for spectrum (a)

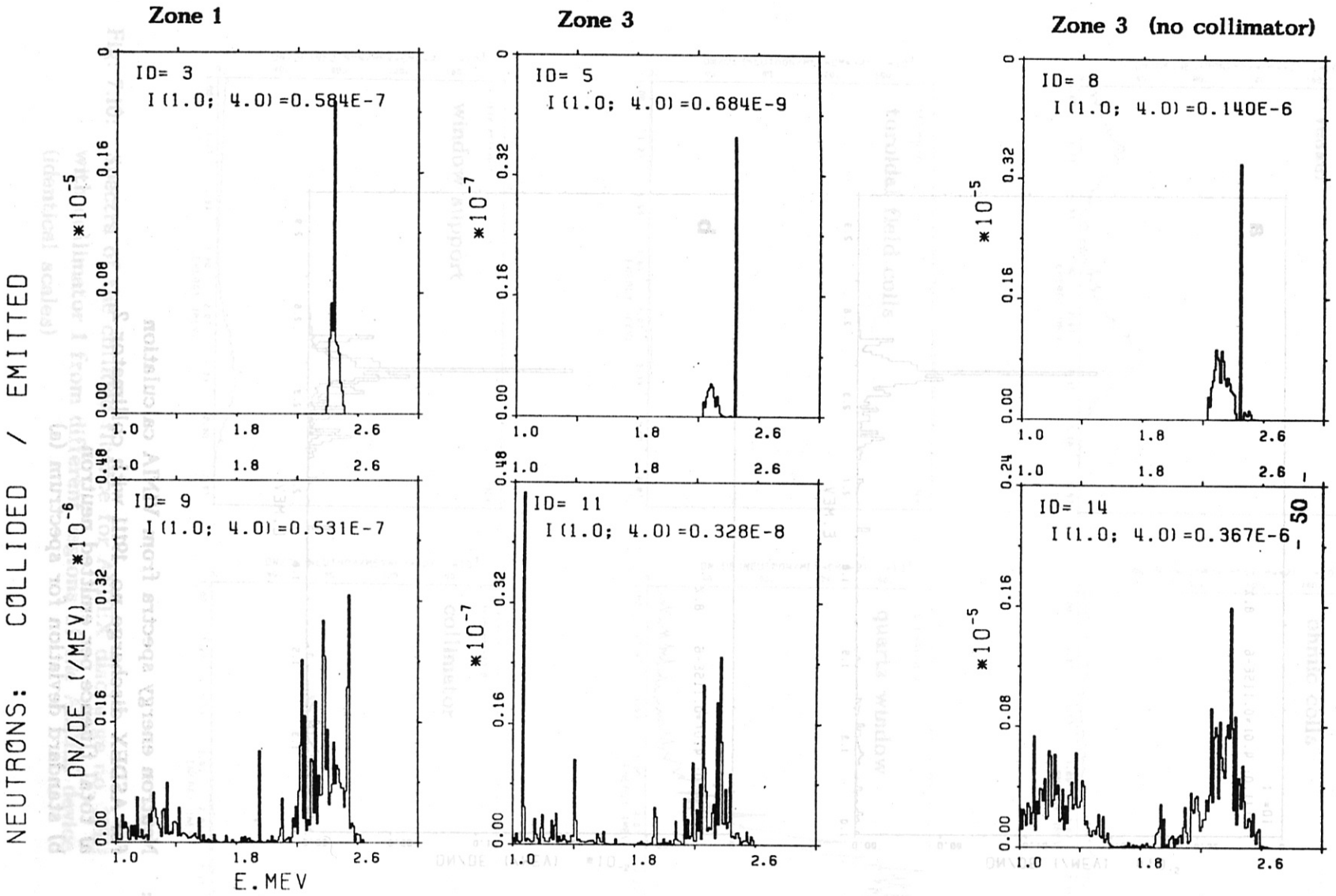

Fig. 8.2: Neutron energy spectra from VINIA calculation for ASDEX discharge no. 19111 with collimator 2, components of spectral fluence at the emulsion for emitted and collided neutrons in the two zones and for zone 3 if no collimator is present

total

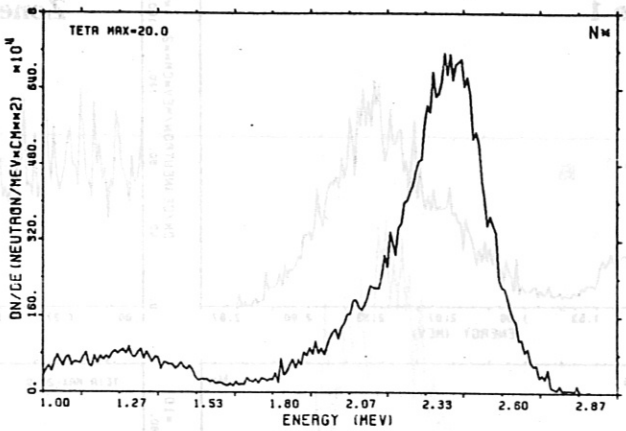

emitted

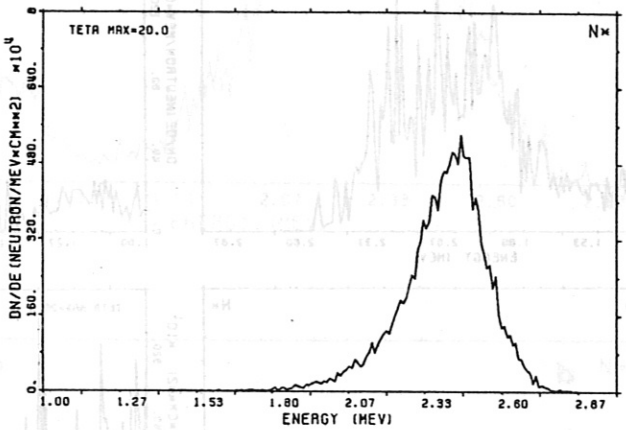

collided

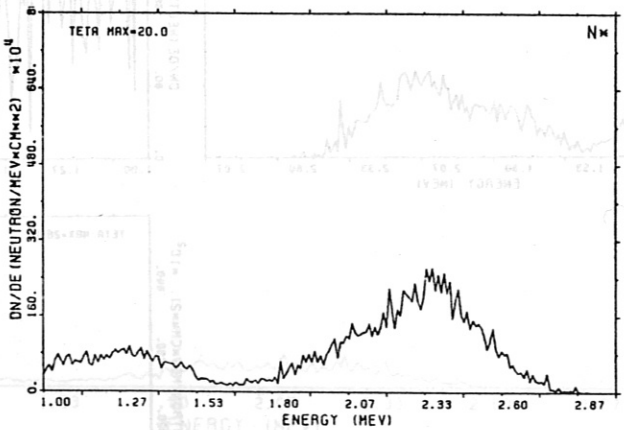

Fig. 8.3: Components of spectral fluence for ASDEX discharge no. 19111 with collimator 2 for all, emitted, and collided neutrons summed over both zones as calculated by NEPMC software using VINIA results

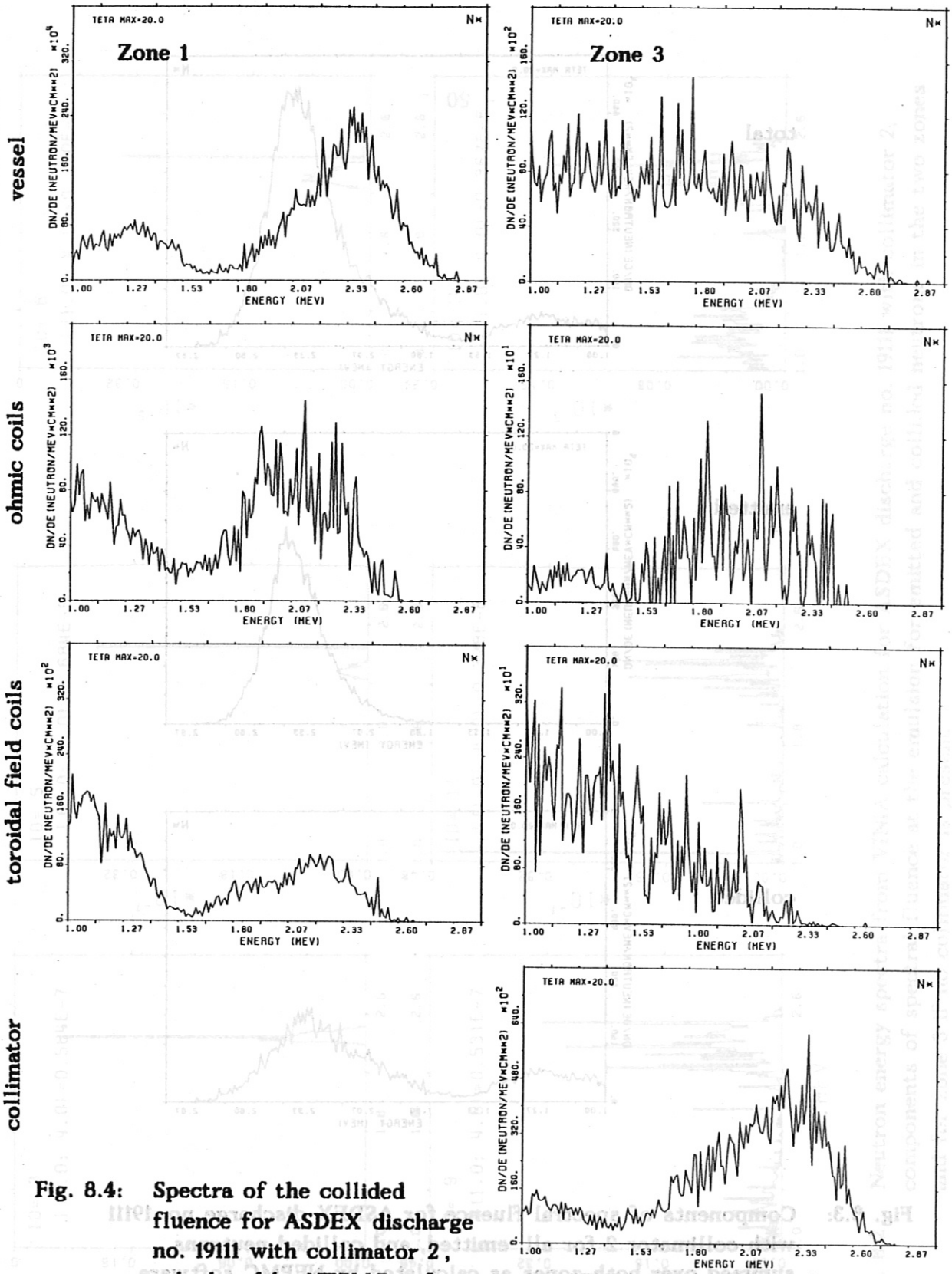

Fig. 8.4: Spectra of the collided fluence for ASDEX discharge no. 19111 with collimator 2, calculated by NEPMC software using VINIA results for both zones from different regions of the ASDEX device (individual scales)

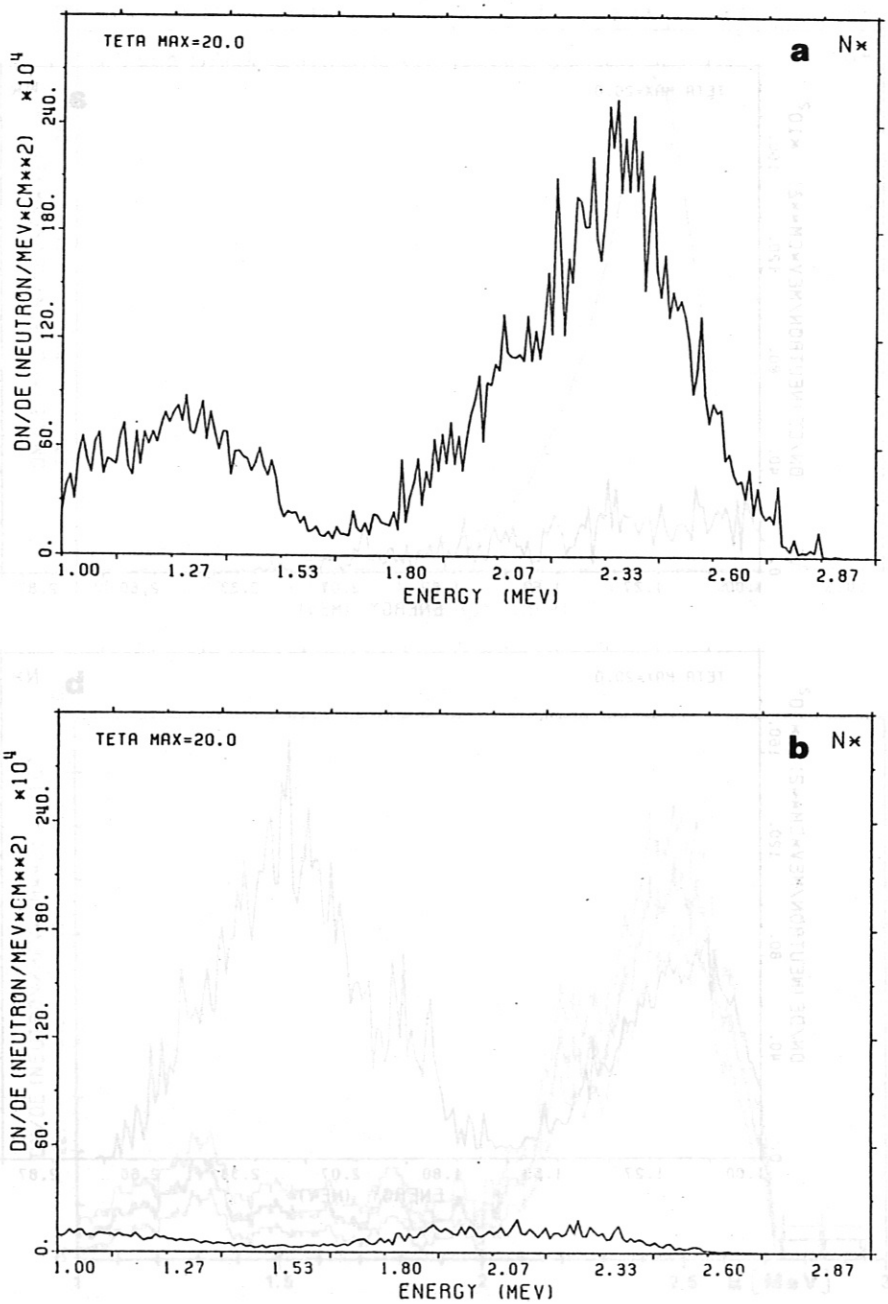

Fig. 8.5: Spectra of the collided fluence for ASDEX discharge no. 19111 with collimator 2 calculated by NEPMC software using VINIA results summed over both zones a) from the vessel b) from all other structural parts

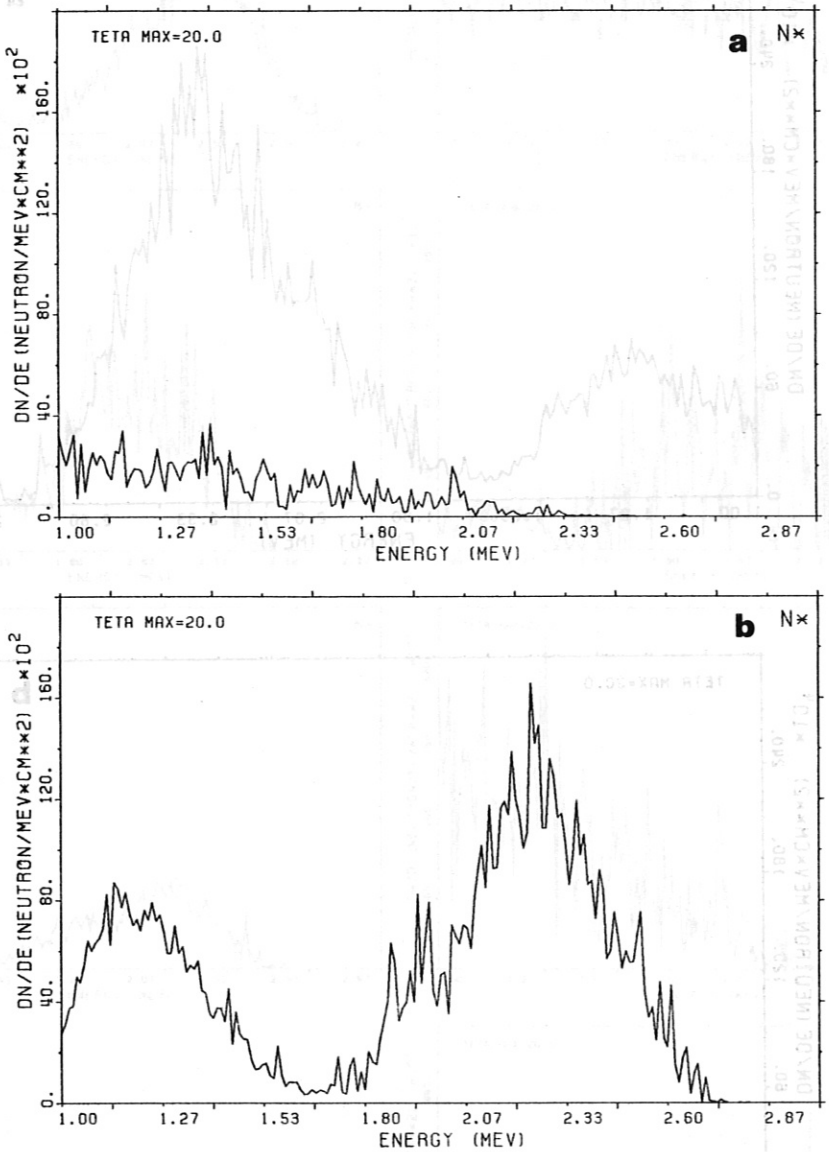

Fig. 8.6: Spectra of the collided fluence from the toriodal field coils for ASDEX discharge no. 19111 with collimator 2, calculated by NEPMC software using VINIA results with (a) and without (b) taking into account the direction of incidence of collided neutrons

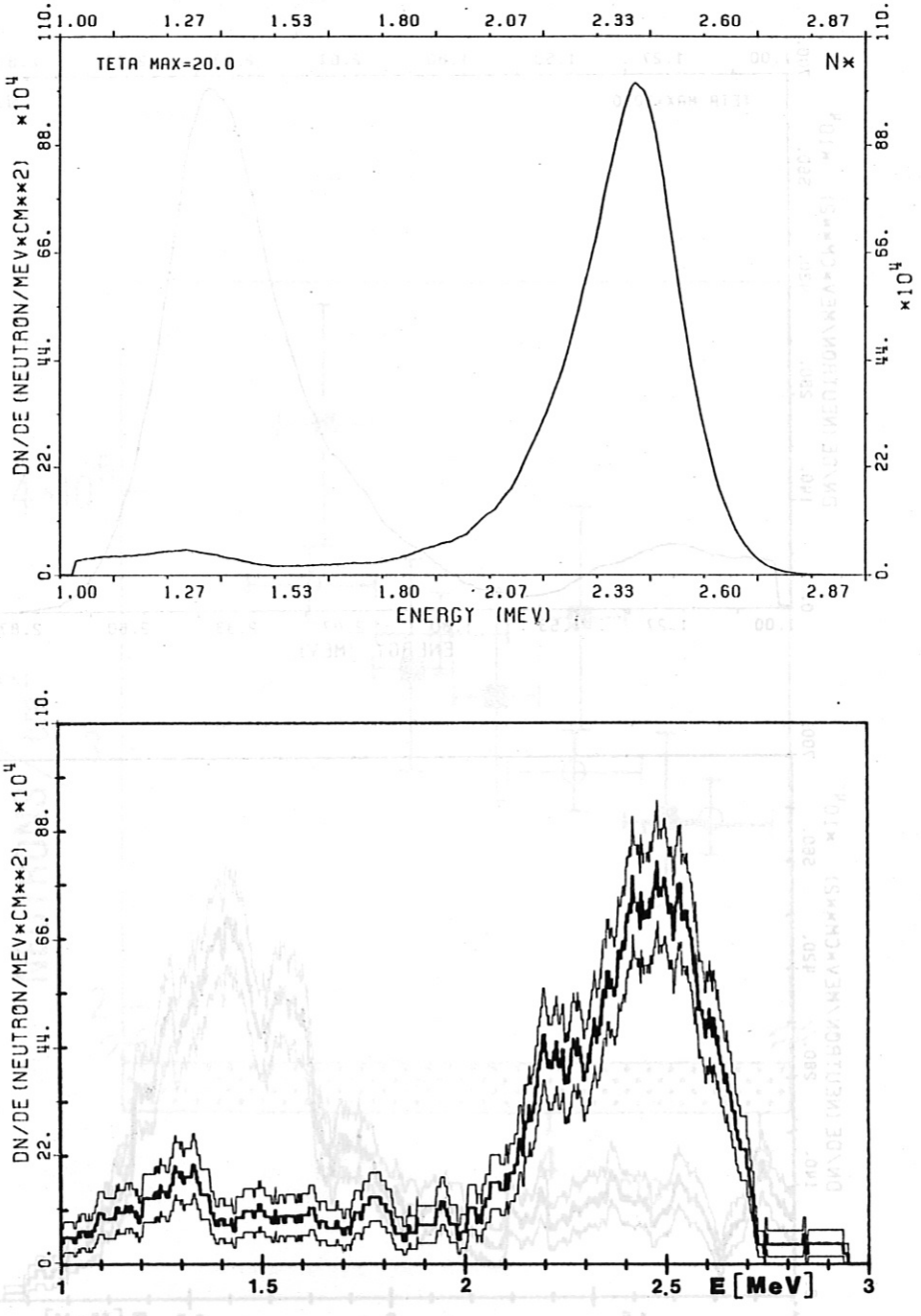

Fig. 9.1: **Neutron energy spectra from NEPMC calculation using VINIA results compared to measured spectra for $\Theta_{max} = 20^0$ for ASDEX discharge no. 16911 with collimator 1. For the measured spectra the lines for one standard deviation are also shown.**

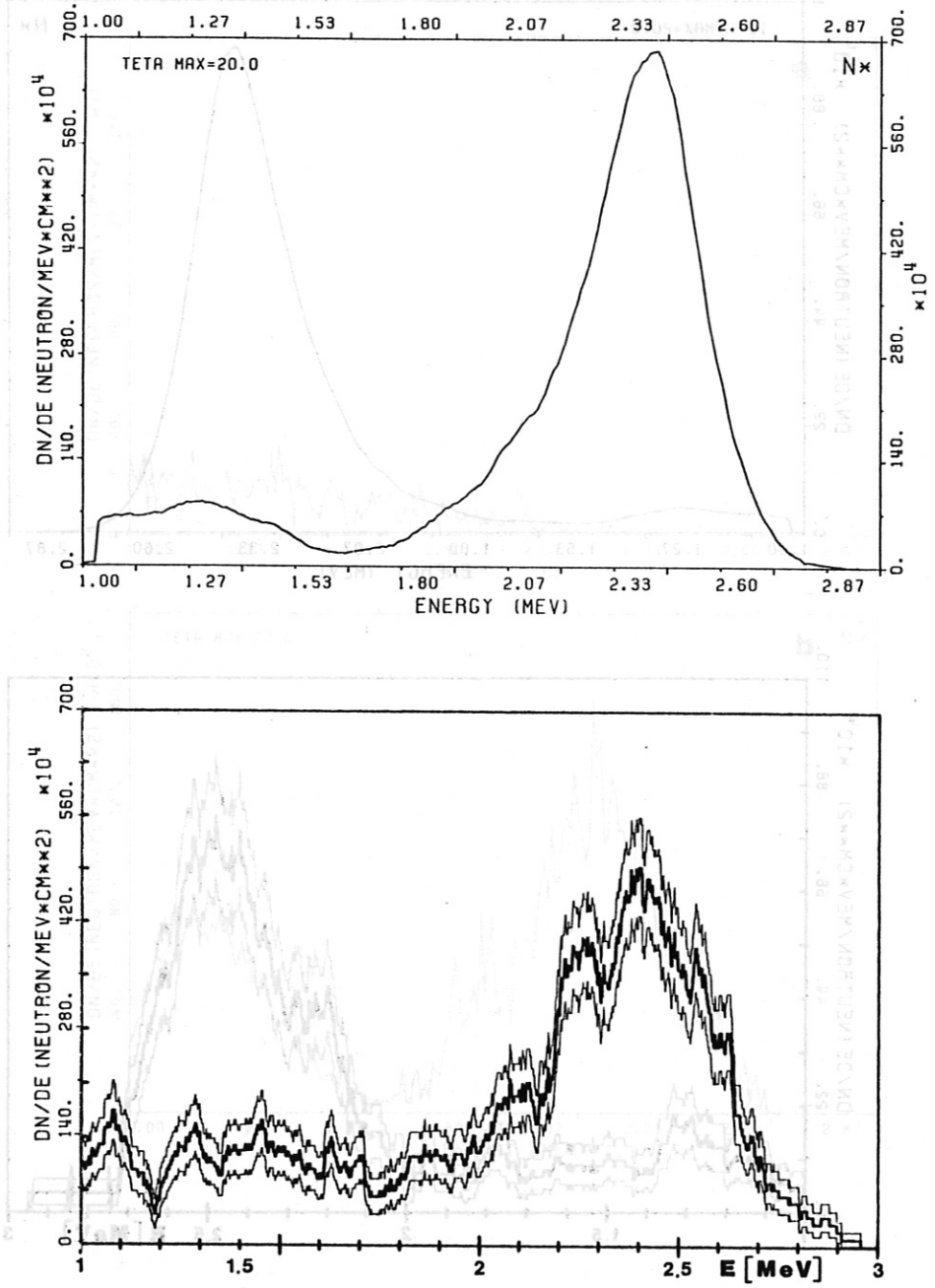

Fig. 9.2: **Neutron energy spectra from NEPMC calculation using VINIA results compared to measured spectra for $\Theta_{max} = 20^0$ for ASDEX discharge no. 19111 with collimator 2. For the measured spectra the lines for one standard deviation are also shown.**

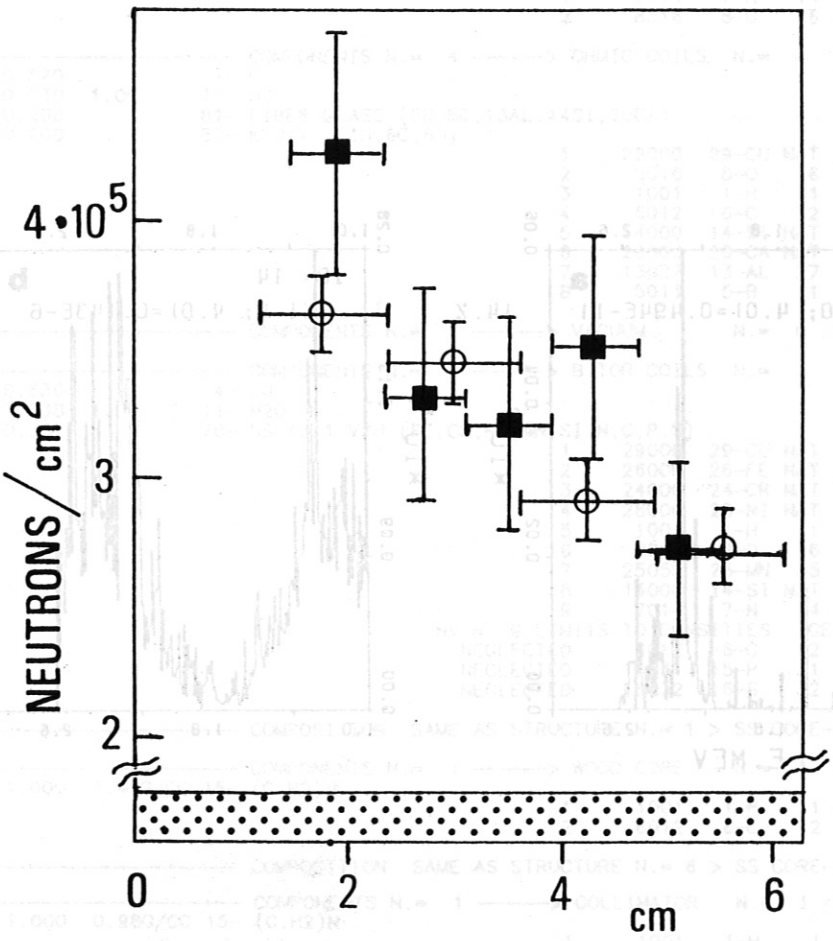

Fig. 9.3: Decrease of neutron flux along emulsion axis for ASDEX discharge no. 16911 with collimator 1, ■ measured values, o values from VINIA calculations

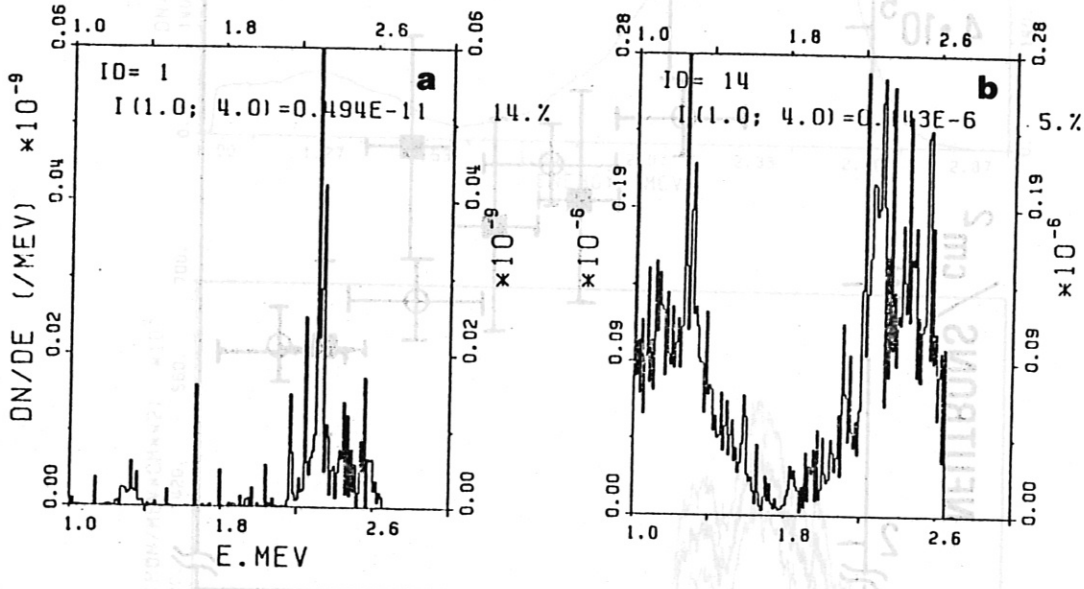

Fig. 10.1: **Neutron energy spectra in the control room (a) compared to the spectrum at the position of collimator 1 (b) inside the hall for ASDEX discharge no. 16911**

```
    ===> NUMBER OF DIFFERENT REGIONS =   14
    ===> NUMBER OF DIFFERENT MATERIALS=   8
REG.
=== INDEX  N  %.VOL  T.D.  INDEX- MATERIAL                    I  NUCLIDE   Z-EL-ISOTOPE NUCLIDES/(BARN*CM)

1).------------------------------ COMPONENTS N.= 1 ------> VACUUM CHAM. N.= 1  SS 4311
   70    9  1.000          70- SS 4311 V2H (FE,CR,NI,MN,SI,N,C,P,S)
                                                  1    26000  26-FE NAT     0.5673E-01
                                                  2    24000  24-CR NAT     0.1601E-01
                                                  3    28000  28-NI NAT     0.8077E-02
                                                  4    25055  25-MN  55     0.1684E-02
                                                  5    14000  14-SI NAT     0.1647E-02
                                                  6     7014   7-N  14     0.5284E-03
                                                  7     6012   6-C  12     0.1155E-03
                                          NV =  7 LIMITS TO DENSITIES  .GE.0.0010*CV(1) <===
                                            NEGLECTED  15031  15-P  31     0.5526E-04
                                            NEGLECTED  16032  16-S  32     0.4328E-04

2).------------------------------ COMPONENTS N.= 1 ------> ROOM SPACE   N.= 1  AIR
   13    2  1.000  1.00ATM. 13- AIR                  T.K = 300.0
                                                  1     7014   7-N  14     0.1957E-04
                                                  2     8016   8-O  16     0.4894E-05

3).------------------------------ COMPONENTS N.= 4 ------> OHMIC COILS  N.= 4
    4    1  0.570           4- CU
   11    2  0.030  1.00     11- H2O
   81    5  0.200          81- FIBER GLASS (5B,8O,13AL,14SI,2OCA)
   82    3  0.200          82- EPOXY  (1H,6C,8O)
                                                  1    29000  29-CU NAT     0.4834E-01
                                                  2     8016   8-O  16     0.1222E-01
                                                  3     1001   1-H   1     0.1141E-01
                                                  4     6012   6-C  12     0.8860E-02
                                                  5    14000  14-SI NAT     0.2740E-02
                                                  6    20000  20-CA NAT     0.1182E-02
                                                  7    13027  13-AL  27     0.8560E-03
                                                  8     5011   5-B  11     0.5900E-03

4).------------------------------ COMPONENTS N.= 0 ------> VACUUM       N.= 0  VACUUM

5).------------------------------ COMPONENTS N.= 3 ------> B.TOR COILS  N.= 3
    4    1  0.630           4- CU
   11    2  0.038  1.00     11- H2O
   70    9  0.332          70- SS 4311 V2H (FE,CR,NI,MN,SI,N,C,P,S)
                                                  1    29000  29-CU NAT     0.5342E-01
                                                  2    26000  26-FE NAT     0.1883E-01
                                                  3    24000  24-CR NAT     0.5316E-02
                                                  4    28000  28-NI NAT     0.2682E-02
                                                  5     1001   1-H   1     0.2543E-02
                                                  6     8016   8-O  16     0.1272E-02
                                                  7    25055  25-MN  55     0.5591E-03
                                                  8    14000  14-SI NAT     0.5468E-03
                                                  9     7014   7-N  14     0.1754E-03
                                          NV =  9 LIMITS TO DENSITIES  .GE.0.0010*CV(1) <===
                                            NEGLECTED   6012   6-C  12     0.3836E-04
                                            NEGLECTED  15031  15-P  31     0.1835E-04
                                            NEGLECTED  16032  16-S  32     0.1437E-04

6).------------------------------ COMPOSITION  SAME AS STRUCTURE N.= 1 > SS CORE-1    N.= -1  SS 4311

7).------------------------------ COMPONENTS N.= 1 ------> WOOD CORE    N.= 1  WOOD
   15    2  1.000  1.40G/CC 15- (C.H2)N
                                                  1     1001   1-H   1     0.1205
                                                  2     6012   6-C  12     0.6023E-01

8).------------------------------ COMPOSITION  SAME AS STRUCTURE N.= 6 > SS CORE-2    N.= -6  SS 4311

9).------------------------------ COMPONENTS N.= 1 ------> COLLIMATOR   N.= 1  CH2
   15    2  1.000  0.98G/CC 15- (C.H2)N
                                                  1     1001   1-H   1     0.8432E-01
                                                  2     6012   6-C  12     0.4216E-01

10).----------------------------- COMPONENTS N.= 1 ------> QUARTZ WINDOW N.= 1  QUARTZ
   14    2  1.000  1.00/QTZ 14- SI.O2
                                                  1     8016   8-O  16     0.5293E-01
                                                  2    14000  14-SI NAT     0.2646E-01

11).----------------------------- COMPOSITION  SAME AS STRUCTURE N.= 1 > V ACUUM CHAM. N.= -1  SS 4311

12).----------------------------- COMPOSITION  SAME AS STRUCTURE N.= 9 > C OLLIMATOR   N.= -9  CH2

13).----------------------------- COMPONENTS N.= 1 ------> ILFORD GLASS N.= 1
   14    2  1.000  1.00/QTZ 14- SI.O2
                                                  1     8016   8-O  16     0.5293E-01
                                                  2    14000  14-SI NAT     0.2646E-01

14).----------------------------- COMPOSITION  SAME AS STRUCTURE N.= 1 > S S DIVERTOR  N.= -1  SS 4311
```

Table 3.1